Institute of
Sustainable Energy

New insights into Environmental and Energy Development

Extended abstracts

4th International Conference on Sustainable Energy and Environmental Development

Institute of
Sustainable Energy

New insights into Environmental and Energy Development

Extended abstracts

4th International Conference on Sustainable Energy
and Environmental Development

EDITORSHIP

Main Editor:	Krzysztof Sornek
Scientific Editors:	Katarzyna Szramowiat-Sala
	Krzysztof Sornek
	Rafał Figaj
	Mateusz Karczewski
Type setting and layout:	Krzysztof Sornek
	Mateusz Karczewski
	Kamila Rzepka
Correction:	Krzysztof Sornek
Cover design:	Krzysztof Sornek

Publishing House:

Institute of Sustainable Energy
31-315 Krakow, Radzikowskiego Str. 100B/43, P: 735 753 110
wydawnictwo@instytutze.org

Cover illustration:
Rawpixel.com, Freepik

4th International Conference on Sustainable Energy and Environmental Development
13-15 October, 2021 | Krakow, Poland

ISBN: 978-83-66559-07-3

Kraków 2021

THE CONTENT

AIR POLLUTION CAUSED BY FIRES AT WASTE STORAGE SITES: ANALYSIS OF SELECTED EPISODES IN POLAND

Tomasz Gorzelnik[1,*]; Robert Oleniacz[1]; Wojciech Drzewiecki[1]; Katarzyna Grzesik[1]; Zbigniew Kowalewski[1]; Ryszard Kozakiewicz[1]; Karolina Kossakowska[1]

[1] AGH University of Science and Technology, Faculty of Mining Surveying and Environmental Engineering, Department of Environmental Management and Protection, Mickiewicza Av. 30, 30-059 Krakow, Poland

* corresponding author: tomaszgo@agh.edu.pl

Abstract. *In this study the impact on air quality of selected fires at waste storage sites in Poland in the last few years was assessed using measurement results derived from the public air quality monitoring (AQM) system, meteorological data, forward trajectory modelling, aerosol optical depth (AOD) data and satellite imagery analysis. The concentrations of selected air pollutants (PM_{10}, $PM_{2.5}$, SO_2, NO_2, NO_x, CO, and C_6H_6) were treated as characteristic substances of waste fires. Taking the wind direction into account enabled to assess whether the concentrations increase at particular station and in a given period might be related to the occurrence of the fire in the vicinity of the measurement point or coincidental. In the situations where the wind was blowing from the place of the fire occurrence to the AQM station, the significant concentration peaks of the analysed substances were observed. The study showed that the fumes from large waste fires spread over a long distance, so that the increase in air pollutant concentrations can be recorded in AQM stations located further away from the fire site. In the layer of the atmosphere where the smoke is transported, its influence on the AOD data from satellite observations was also visible.*

Keywords: *waste fires, air quality, high concentration episodes, forward trajectory modelling, aerosol optical depth.*

1 Introduction

In Poland, a very large number of cases of waste fires have been observed in recent years, among which approx. 200-400 per year are classified as at least medium fires, and several dozen per year are large and very large fires [1]. These fires usually occur in waste storages and landfills (including illegal ones), due to a large number of such facilities in Poland [2,3], a significant amount of municipal solid waste sent to mechanical-biological treatment (MBT) installations and installations producing refuse-derived fuel (RDF) with consideration of limited capacity of waste recycling facilities, waste incineration and waste co-incineration plants [2,4], and primarily the increasing costs of waste management and the ban on importing waste paper and plastic introduced by China [5,6]. Comprehensive survey of waste collection and storage companies in

Sweden, carried out by Ibrahim et al. [7] in 2010, also showed some correlation between the frequency of waste fires and the type of material recycled in recent years.

A waste fire, regardless of its cause, contributes to various environmental influences: ecological (through emissions of pollutants into the environment), economic (losses of energy and recyclable materials, extinguishing costs) and social (through redirection of taxes to recuperation of resources and/or the environment or by impact on health of citizens exposed to emissions) [8-10]. In a similar way to any open and uncontrolled incineration of waste, the accompanying emission of significant amounts of pollutants to the air may be a serious environmental problem. These pollutants are: particulate matter (PM) containing soot and heavy metals, carbon monoxide (CO), methane (CH_4) and other light hydrocarbons, volatile organic compounds (VOCs) such as e.g. benzene (C_6H_6), semi-volatile organic compounds (SVOCs) such as e.g. polycyclic aromatic hydrocarbons (PAHs), polychlorinated biphenyls (PCBs) and polychlorinated dibenzo-*p*-dioxins/furans (PCDD/PCDFs) [11-13], and in some cases also acidic gaseous pollutants such as: sulphur dioxide (SO_2), nitrogen oxides (NO_x), hydrogen cyanide (HCN) or hydrogen chloride (HCl) [14,15]. The main purpose of this study is to present the impact of selected large fires at waste storage sites in Poland in 2018-2021 on the measurement results of air pollutant concentrations, taking into account the wind direction. The purpose was also to check whether the impact is also reflected in aerosol optical depth (AOD) data, as in the case of a larger scale biomass burning and forest or vegetation fires [16-18].

2 Materials and Methods

The research covered three examples of fires taking place at points of collection, storage and processing of such waste as: waste electrical and electronic equipment, metal scrap, plastic packaging and waste paper along with machines for their shredding (Szczecin, 20.09.2018), waste tyres and plastics (Żory, 28.11-4.12.2018), as well as used tyres together with the warehouse hall of the vulcanization plant (Lubrza, 2.06.2021). From 34 to 43 units of the fire brigade participated in extinguishing these fires. The impact of these fires on the air quality was assessed with the use of data derived from the nearest air quality monitoring (AQM) stations [19], where a significant increase of the pollutants concentration (associated with a given fire) was recorded during the fire. These concentrations were averaged over the period of this increase and compared with the background of pollutants occurring in the corresponding time interval (in the same hours) 1 day earlier.

At the initial stage of identifying the monitoring stations exposed to pollution resulting from fire, the direction and speed of the wind as well as their variability over time were taken into account. Data from meteorological stations of the Institute of Meteorology and Water Management – National Research Institute in Szczecin, Racibórz and Opole [20], the results of forward trajectory modelling using the HYSPLIT model [21] and satellite imagery from the Sentinel 2 and Planet Dove satellites were used. For each waste fire episode HYSPLIT forward trajectory modelling was performed on three starting height levels: 10, 100 and 500 m above ground level. The input meteorological data were derived from NCAR/NCEP 2.5-degree global reanalysis archive from the ARL server. The changes in AOD values were assessed based on the MAIAC (Multiangle Implementation of Atmosheric Correction) AOD product (MCD19A2 V6) derived from combined Terra and Aqua satellites MODIS (Moderate Resolution Imaging Spectroradiometer) sensor data [22]. AOD at 0.47 μm and AOD at 0.55 μm are among the layers of this gridded Level 2 product produced daily at 1 km resolution. The MAIAC AOD product was downloaded from NASA's Level-1 and Atmosphere Archive and Distribution System (LAADS) Distributed Active Archive Center (DAAC) [23].

3 Results

The forward trajectories for the analysed fires of waste storage sites along with marked AQM stations and ground meteorological stations of the Institute of Meteorology and Water Management are presented in Fig. 1. Table 1 presents a comparison of the average concentrations of pollutants recorded at AQM stations in the period of their significant increase during the occurrence of fires and assumed as background, as well as the meteorological conditions occurring at that time.

The data presented in Table 1 show that at the AQM stations, located within the range of impact of smoke from the analysed fire cases, a significant, often multiple increase of the concentration of some pollutants (including PM_{10}, $PM_{2.5}$, NO_x, CO i C_6H_6, and in the case of the waste tyres also SO_2) was recorded. This increase was greater when the pollutant plume moved towards a given station and approached the ground surface. On the other hand, in the case of stations located relatively close to the place of fire (e.g. Żory and Szczecin-1), possible increases in concentration are smaller due to the rapid rising up of the smoke.

The highest observed concentrations of PM_{10} (above the alarm level of 300 $\mu g/m^3$), as well as SO_2, CO and C_6H_6, took place at the AQM station in Rybnik during the largest of the analysed waste fires (in Żory). The extinguishing operation lasted over 6 days, and the background of pollution was increased due to the heating season and low temperatures. Significant increases and decreases of concentrations were observed periodically depending on changes of wind speed and direction (the extreme case was taken into account in Table 1). Thus, for the station in Rybnik, the concentration values from the initial period of the fire could be adopted as the pollution background, because the wind was blowing in a different direction at that time.

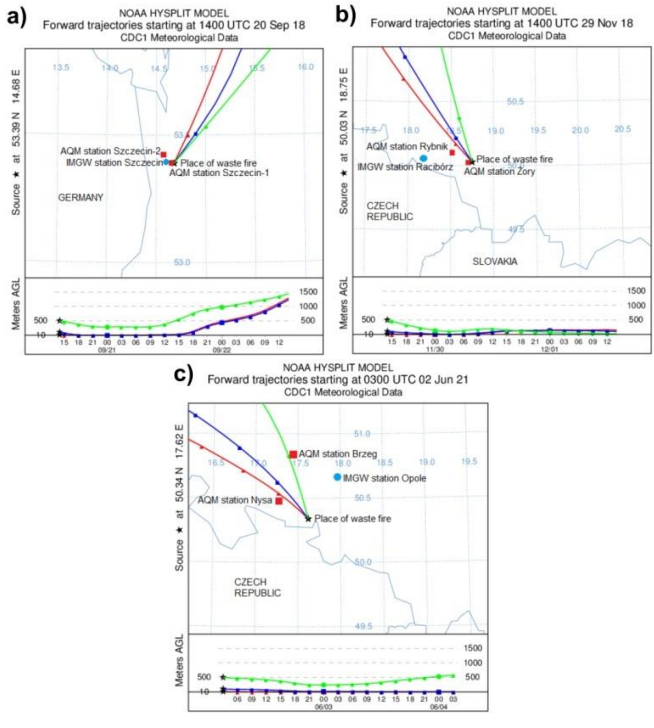

Fig. 1. Results of HYSPLIT forward trajectories modelling for the analysed waste fire episodes in Poland: a) Szczecin (20.08.2018, 14:00 UTC), b) Żory (29.11.2018, 14:00 UTC), c) Lubrza (2.06.2021, 03:00 UTC).

Table 1. Average values of air pollutant concentrations and meteorological data for the analysed fire episodes and the background periods (in brackets - the ratio of concentrations from the fire episode to the background).

Location and time of fire broke out	**Szczecin 20.09.2018 approx. 14:00 (UTC)**		**Żory 28.11.2018 approx. 00:00 (UTC)**		**Lubrza 2.06.2021 approx. 03:00 (UTC)**	
AQM station	**Szczecin-1**	**Szczecin-2**	**Żory**	**Rybnik**	**Nysa**	**Brzeg**
Distance, km	2	10	4	19	24	58
Azimuth deg.	230	297	270	299	303	349
Date, hours - fire episode / background	20.09.18 / 19.09.18, 17:00-19:00	20.09.18 / 19.09.18, 17:00-22:00	28.11.18 / 27.11.18, 00:00-07:00	29-30.11.18 / 28-29.11.18, 16:00-10:00	2.06.21 / 1.06.21, 05:00-07:00	2.06.21 / 1.06.21, 04:00-06:00
PM_{10}, µg/m^3	90.3 / 43.3 (2.1)	-	-	307.0 / 58.8 (5.2)	40.9 / 21.8 (1.9)	38.9 / 22.9 (1.7)
$PM_{2.5}$, µg/m^3	16.8 / 13.8 (1.22)	36.2 / 19.4 (1.9)	-	-	21.2 / 8.7 (2.4)	29.4 / 16.0 (1.8)
SO_2, µg/m^3	2.5 / 2.3 (1.09)	4.5 / 3.9 (1.15)	33.4 / 9.6 (3.5)	43.6 / 14.4 (3.0)	-	-
NO_2, µg/m^3	48.1 / 45.1 (1.05)	115.0 / 49.6 (2.3)	-	48.3 / 28.7 (1.7)	-	25.0 / 25.9 (0.97)
NO_x as NO_2, µg/m^3	53.0 / 49.7 (1.07)	262.5 / 58.9 (4.5)	-	121.5 / 37.5 (3.2)	-	-
CO, mg/m^3	-	1.08 / 0.42 (2.6)	0.94 / 0.37 (2.5)	1.64 / 0.47 (3.5)	-	-
C_6H_6, µg/m^3	-	3.9 / 0.82 (4.8)	-	15.8 / 3.7 (4.2)	-	2.1 / 0.50 (4.2)
Surface wind direction	ESE / SE (Szczecin)	SE / SSW (Szczecin)	NNE / NNE (Racibórz)	SE-SSW / E (Racibórz)	SE / W (Opole)	SE / SSW (Opole)
Surface wind speed, m/s	1.5 / 2.5	1.0 / 2.6	3.3 / 4.6	5.4 / 1.8	4.0 / 1.5	2.5 / 1.0
Temp., ºC	18.5 / 18.8	16.1 / 19.4	-1.4 / -0.8	-1.9 / -4.2	17.5 / 13.4	15.7 / 10.8

The analysis of the modelled forward trajectories performed for the episode of a fire in Lubrza (Fig. 1c) suggests that the brief increase of pollutant concentrations at the stations in Nysa and Brzeg in the morning of 2.06.2021 could correspond to this rather intense, but relatively short-term fire (it was extinguished within a few hours). The effects of the fire can therefore be observed even at such a large distance from its place, and the increase in C_6H_6 concentrations in Brzeg compared to the previous day's background is comparable to the situation that took place at AQM stations in Szczecin or Rybnik in the case of much closer fires. However, taking into account the absolute values of the measured concentrations, if the fire in Lubrza happened at a higher background pollution level (e.g. during heating season), it would rather not be noticeable at more distant monitoring stations.

An attempt was also made to assess the impact of the analysed waste fires on the aerosol optical depth (AOD) at 0.47 µm, estimated on the basis of satellite observations of the MODIS sensor (MCD19A2 product). This influence was especially visible in the case of the fire in Żory (Fig. 2). Unfortunately, due to the weather conditions, the last pre-fire estimate of the AOD value for the research area, available for this product, was from 17.11.2018 (Fig. 2a), so it precedes the

fire by 11 days. Nevertheless, this estimation was taken as a view of the air pollution in the absence of the impact caused by the fire. On the other hand, products based on the images recorded on 29.11.2018 (Fig. 2c) and 30.11.2018 (Fig. 2d), i.e. on the second and third day of the fire, were available. According to the analysis of satellite data, the average value of AOD in the atmosphere layer over Rybnik and Żory on 29.11.2018 at 12:00, increased by approximately 69% and 82%, respectively, compared to the observation on 17.11.2018 at 11:35. The AOD value estimated for cells with measuring stations in Rybnik and Żory increased by 53% and 127%, respectively. The AOD increase rate was therefore lower than the increase in the average concentration of particulate matter PM10 in the Rybnik AQM station shown in Table 1.

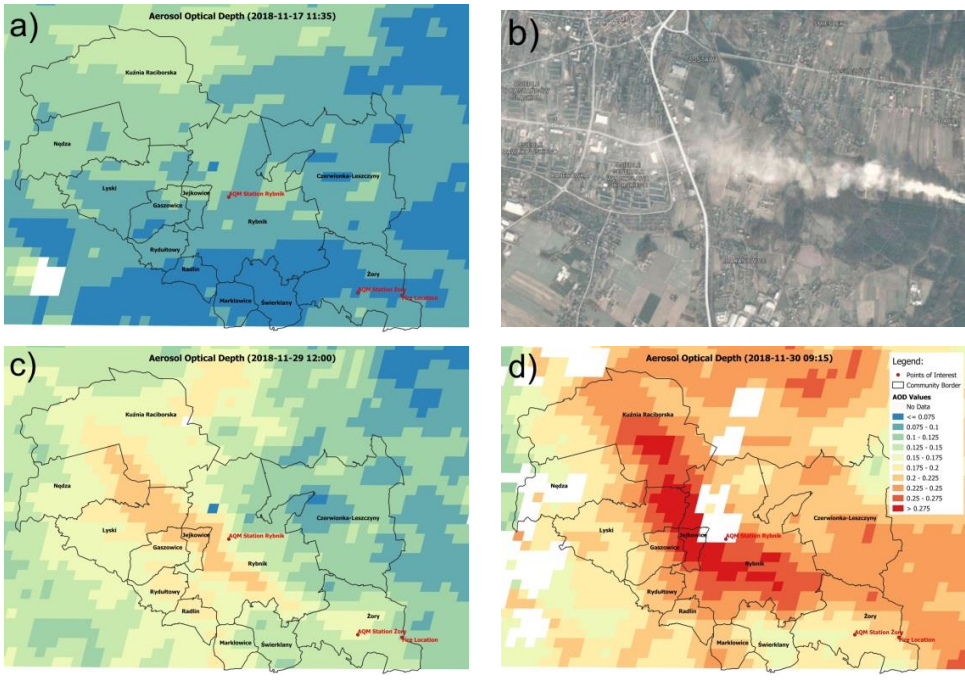

Fig. 2. Satellite products used in the study: a) MODIS AOD (17.11.2018, 11:35 UTC), b) Planet Dove image (29.11.2018, 9:18 UTC), c) MODIS AOD (29.11.2018, 12:00 UTC), d) MODIS AOD (30.11.2018, 9:15 UTC) (source: own work based on data from NASA, Planet, OSM and Polish Head Office of Geodesy and Cartography)

Due to the very long duration of the extinguishing of waste fire in Żory and the changing wind direction, the atmospheric air was polluted with smoke over a large area. This was reflected in the spatial distributions of AOD values observed on 29.11.2018 and 30.11.2018 (Fig. 2c and d). The area of AOD values increased in relation to the surrounding terrain is visible in the form of a plume spreading from the city of Żory in the north-west direction, covering the southern and eastern part of Rybnik and partially the adjacent communities. This direction of pollution spread is also confirmed by the plume visible directly on the high-resolution satellite image recorded on 29.11.2018 (Fig. 2b).

In the case of fires in Szczecin and Lubrza, these events, due to the time and duration of their occurrence, were not recorded on high-resolution satellite images. However, for the region of Szczecin, there are available MODIS products showing AOD values in the areas where the AQM stations are located immediately before the fire (20.09.2018, 12:40 UTC) and in the morning of the next day (21.09.2018, 9:55 UTC). They show an increase in the AOD value for the Szczecin-2 station area by 36% and for the Szczecin-1 station area by 16%. In turn, for a fire in Lubrza, the

nearest AOD registrations from the MODIS sensor come from 1.06.2021, 11:45 UTC (before the fire) and 2.06.2021, 10:40 UTC (after the fire). The AOD values for the AQM stations in Nysa and Brzeg increased by 125% and 68%, respectively. Both in the case of Szczecin and Lubrza, it was not possible to indicate the boundaries of the area of significant air pollution caused by the analysed fires (too many areas without an estimated AOD value due to the presence of clouds).

4 Conclusions

The analysed episodes of fire in waste storage sites caused periodic significant air pollution by substances typical for open combustion processes, which confirms the results of other studies on large fires in landfills [24,25]. In the case of a fire generating a large amount of smoke, it usually spreads at a certain height above the ground. Therefore, the concentrations of pollutants recorded at nearby AQM stations come from the plume significantly diluted with air and they are not as high as they could be if the plume moved in the near-surface layer. However, the fact that the air quality deteriorates several times at stations located at different distances from the fire indicates a large scale of the potential impact of this type of emission source. Such substances as PM_{10}, $PM_{2.5}$, NO_x, CO and C_6H_6, which are quite often measured in Poland at AQM stations [19,26], can be appropriate air pollution indicators. In case of the availability of appropriate satellite data the aerosol optical depth (AOD) can be a useful air pollution indicator as well.

Acknowledgements

This research was funded by the grant "Excellence initiative - research university" for the AGH University of Science and Technology, grant no. 501.696.7996. The Authors acknowledge Planet Education and Research Program for free access to Planet Dove imagery used in this study. In this research there were used and processed data from the Institute of Meteorology and Water Management – National Research Institute.

References

[1] Bihałowicz JS, Rogula-Kozłowska W, Krasuski A. Contribution of landfill fires to air pollution - An assessment methodology. Waste Management 2021;125;182-91; DOI: 10.1016/j.wasman.2021.02.046.

[2] Jakubus M, Stejskal B. Municipal solid waste management systems in Poland and the Czech Republic. A comparative study. Environment Protection Engineering 2020;46(3);61-78; DOI: 10.37190/epe200304.

[3] Król S. Illegal landfill sites in Poland. World Scientific News 2016;48;164-70.

[4] Malinauskaite J, Jouhara H, Czajczyńska D, Stanchev P, Katsou E, Rostkowski P et al. Municipal solid waste management and waste-to-energy in the context of a circular economy and energy recycling in Europe. Energy 2017;141;2013-44; DOI: 10.1016/j.energy.2017.11.128.

[5] Ma Z, Yang Y, Chen WQ, Wang P, Wang C, Zhang C et al. Material flow patterns of the global waste paper trade and potential impacts of China's import ban. Environmental Science & Technology 2021;55;8492-501; DOI: 10.1021/acs.est.1c00642

[6] Li C, Wang L, Zhao J, Deng L, Yu S, Shi Z et al. The collapse of the global plastic waste trade: Structural change, a cascading failure process and potential solutions. Journal of Cleaner Production 2021;127935; DOI: 10.1016/j.jclepro.2021.127935.

[7] Ibrahim MA, Alriksson S, Kaczala F, Hogland W. Fires at storage sites of organic materials, waste fuels and recyclables. Waste Management & Research 2013;31(9);937-45; DOI: 10.1177/0734242X13487581.

[8] Stenis J, Hogland W. Fire in waste-fuel stores: risk management and estimation of real cost. Journal of Material Cycles and Waste Management 2011;13(3);247-58; DOI: 10.1007/s10163-011-0013-1. DOI: 10.1016/j.renene.2020.05.021.

[9] Ibrahim MA. Risk of spontaneous and anthropogenic fires in waste management chain and hazards of secondary fires. Resources, Conservation and Recycling 2020;159;104852; DOI: 10.1016/j.resconrec.2020.104852.

[10] Mikalsen RF, Lönnermark A, Glansberg K, McNamee M, Storesund K. Fires in waste facilities: Challenges and solutions from a Scandinavian perspective. Fire Safety Journal 2021;120;103023; DOI: 10.1016/j.firesaf.2020.103023.

[11] Lemieux PM, Lutes CC, Santoianni DA. Emissions of organic air toxics from open burning: a comprehensive review. Progress in Energy and Combustion Science 2004;30(1);1-32; DOI: 10.1016/j.pecs.2003.08.001.

[12] Lönnermark A, Blomqvist P, Marklund S. Emissions from simulated deep-seated fires in domestic waste. Chemosphere 2008;70(4);626- 39; DOI:10.1016/j.chemosphere.2007.06.083.

[13] Estrellan CR, Iino F. Toxic emissions from open burning. Chemosphere 2010;80(3);193-207; DOI: 10.1016/j.chemosphere.2010.03.057.

[14] Downard J, Singh A, Bullard R, Jayarathne T, Rathnayake CM, Simmons DL et al. Uncontrolled combustion of shredded tires in a landfill - Part 1: Characterization of gaseous and particulate emissions. Atmospheric Environment 2015;104;195-204; DOI: 10.1016/j.atmosenv.2014.12.059.

[15] Stockwell CE, Yokelson RJ, Kreidenweis SM, Robinson AL, DeMott PJ, Sullivan RC et al. Trace gas emissions from combustion of peat, crop residue, domestic biofuels, grasses, and other fuels: configuration and Fourier transform infrared (FTIR) component of the fourth Fire Lab at Missoula Experiment (FLAME-4). Atmospheric Chemistry and Physics 2014;14(18);9727-54; DOI: 10.5194/acp-14-9727-2014.

[16] Chen J, Li C, Ristovski Z, Milic A, Gu Y, Islam MS et al. A review of biomass burning: Emissions and impacts on air quality, health and climate in China. Science of the Total Environment 2017;579;1000-34; DOI: 10.1016/j.scitotenv.2016.11.025.

[17] Zhu Q, Liu Y, Jia R, Hua S, Shao T, Wang B. A numerical simulation study on the impact of smoke aerosols from Russian forest fires on the air pollution over Asia. Atmospheric Environment 2018;182;263-74; DOI: 10.1016/j.atmosenv.2018.03.052.

[18] Reddington CL, Conibear L, Robinson S, Knote C, Arnold SR, Spracklen DV. Air pollution from forest and vegetation fires in Southeast Asia disproportionately impacts the poor. GeoHealth 2021;e2021GH000418; DOI: 10.1029/2021GH000418.

[19] Portal jakości powietrza GIOŚ, http://powietrze.gios.gov.pl/pjp/current [accessed 31.08.2021].

[20] IMGW-PIB public data, https://danepubliczne.imgw.pl [accessed 31.08.2021].

[21] Stein AF, Draxler RR, Rolph GD, Stunder BJB, Cohen MD, Ngan F. NOAA's HYSPLIT atmospheric transport and dispersion modeling system. Bulletin of the American Meteorological Society 2015;96;12; DOI: 10.1175/BAMS-D-14-00110.1.

[22] Lyapustin A, Wang Y, Korkin S, Huang D. MODIS collection 6 MAIAC algorithm. Atmospheric Measurement Techniques 2018;11;5741-5765; DOI: 10.5194/amt-11-5741-2018.

[23] https://ladsweb.modaps.eosdis.nasa.gov/search/order/2/MCD19A2–6 [accessed 31.08.2021]

[24] Rim-Rukeh A. An assessment of the contribution of municipal solid waste dump sites fire to atmospheric pollution. Open Journal of Air Pollution 2014;3(03);53; DOI: 10.4236/ojap.2014.33006.

[25] Bihałowicz JS, Rogula-Kozłowska W, Krasuski A, Salamonowicz Z. The critical factors of landfill fire impact on air quality. Environmental Research Letters 2021; in press DOI: 10.1088/1748-9326/ac27cd.

[26] Oleniacz R, Gorzelnik T. Assessment of the variability of air pollutant concentrations at industrial, traffic and urban background stations in Krakow (Poland) using statistical methods. Sustainability 2021;13;5623; DOI: 10.3390/su13105623.

WASTE FIRES – WASTE OF ENERGY, WASTE OF MATERIALS

Katarzyna Grzesik[1,*]; Karolina Kossakowska[1]; Ryszard Kozakiewicz[1]; Zbigniew Kowalewski[1]; Tomasz Gorzelnik[1]; Robert Oleniacz[1]; Wojciech Drzewiecki[1]

[1] AGH University of Science and Technology, Faculty of Mining Surveying and Environmental Engineering, Department of Environmental Management and Protection, Mickiewicza Ave. 30, 30-059 Krakow, Poland

* corresponding author: grzesikk@agh.edu.pl

Abstract. *In 2018, there were 243 fires in waste management facilities in Poland, and in 2019, the number of waste fires amounted to 176. During the uncontrolled incineration of waste, the environment is significantly polluted through the emission of toxic substances to the air, water and soil, and various compounds are leached out of the combustion residues. In addition to the negative environmental aspects, waste fires cause enormous losses of materials, that could be recycled or recovered. Therefore the waste fires directly affect the depletion of natural resources. According to the waste hierarchy, if the recycling is not feasible, waste should be recovered, for example for energy generation purposes. Considering that fires burn waste with high calorific value, there is a loss of energy that could be obtained from waste in incineration plants or in cement plants fuelled by RDF (refuse derived fuel). In the paper detailed data on waste fires in recent years in Poland have been summarized, taking into account the location and size of fires, type of waste management facilities in which fires occurred. The paper also shows types of waste that were fired. Moreover the an estimation of amount of waste that was burned was done and thus their material and energy value was irretrievably lost.*

Keywords: *waste management, open-fires, waste facilities, material losses, energy losses,*

1 Introduction

The total weight of waste generated in Poland in recent years is at the level of about 125-140 million Mg annually and at the level of 12-13 million Mg of municipal waste [1]. Unfortunately not all waste is treated or disposed properly.

At the same time more and more stringent waste management law regulations have been introduced. Directive 1999/31/EC on the landfill of waste [2] introduced restrictions on the disposal of biowaste in landfills. In 2008 waste framework directive [3] ordered 50% recycling of paper, glass metal and plastic from household. This directive was implemented in Poland in 2012 in the Act on waste [4]. In 2015 European Commission adopted first Circular Economy Action Plan [5] setting the higher recycling targets: 55% of municipal waste by 2025; 60% by 2030 and 65% by 2035, 65% of packaging waste by 2025, and 70% by 2030. In Poland, since 2016, landfilling of municipal waste or post processing waste with higher calorific value than 6MJ/kg has been banned [6].

On the other hand National Waste management Plan 2022 [7] as one of the main problems indicates insufficient number of waste treatment facilities especially incineration plants. The above premises led to a situation in which municipal waste could not be landfilled and at the same time there were not enough installations (only one incinerator in Warsaw), where they could be recovered into energy. Therefore, a rapid development of mechanical-biological treatment (MBT) plants has been observed since 2012. This type of facility could receive the status of regional installation, where mixed municipal waste could be processed. The main output of MBT is refuse-derived fuel (RDF), which is mainly recovered (incinerated) in cement plants. However, the RDF produced from mixed municipal waste was characterised by low quality, often not accepted by cement plants. As a consequence waste management sector generated a high calorific value waste - RDF of poor quality, for which it was difficult to find the recipient.

There has been additional problem of increasing amounts of imported waste to Poland and at the same time China has stopped importing plastic waste from Europe. The cost of plastic recycling is high, so the revenue from final product – plastic regranulate, does not often cover the real costs of recycling. In this situation, the waste fire has become a "solution" in waste treatment facilities or in waste storage sites. Indeed, in recent years rapid and significant increase of waste fires number has been observed in Poland, reaching the maximum in 2018 – 2019. Waste fires besides causing undoubtedly substantial air pollution, which was proven in numerous studies [8-11], also cause material and energy losses. Recyclables could have been processed into valuable secondary raw materials, and the remaining waste could have been processed and then fuelled, saving non-renewable resources.

In the paper detailed data on waste fires in 2018-2019 in Poland have been summarized, taking into account the location and size of fires, type of waste facilities in which fires occurred. The paper also shows waste types that burned, moreover an estimation of burned waste amount was done. Due to waste fires material and energy value of waste was irretrievably lost.

2 Materials and methods

For the first time data on waste fires was published in Environment 2018 report by Statistics Poland [12], showing the number of landfill fires since 2012. The data on waste fires in waste storage sites were consequently published in Environment 2019 and 2020 [13,1]. However, the primary source of data on waste fires indicated by Statistics Poland is National Headquarters of the State Fire Service (NHSFS).

Therefore for the purpose of this study we asked NHSFS for data on waste fires for 2018 and 2019. We wanted to know: address, date of fire, fire surface, fire-fighting action (duration, number of units taking part in action, used extinguishing media), waste facility, type of burned, quantity, volume of burned waste for each fire. We received detailed data on fire-fighting actions, time and surface of fire. The NHSFS classifies fires into small, medium, large and very large. Criteria for the classification of fires due to size are shown in table 1.

Table 1. Criteria for the classification of fires due to size [14].

Fire size	**Facilities or their part, goods, material storages, machines equipment, raw materials, fuels**	
	Surface [m^2]	**Volume [m^3]**
Small	<70	<350
Medium	71-300	351-1500
Large	301-1000	1501-5000
Very large	>1001	>5001

However, we did not received any data on quantity or volume of burned waste. Moreover, Fire Brigades are not professionals in waste management, thus as facility we often found just 'garbage' or 'garbage dump'. We also asked Chief Inspectorate of Environmental Protection (CIEP) for the data on waste fires for 2018 and 2019. From this institution we received data with waste facility names and types of burned waste for most cases. But still we did not receive any data on quantity, volume of burned waste, either no data was provided on surface size of fire, so we did not know which fire was large, very large, medium or small. Additionally, the number of waste fires or their addresses or their dates were not compatible with the data from NHSFS. However, we took large and very large fires from NHSFS data and compared them with CIEP data, taking into account that there could be slight differences in locations and dates. It turned out that the second institution gives data only for large and very large fires without specifying their surface. Thanks to this comparison we gain insight into types of waste facilities or storage sites or illegal dump sites as well as types of combusted waste for most cases.

In the next step we wanted to calculate the amount of each type of waste that burned. We calculated the total fire surface for each type waste for 2018 and 2019 for large and very large fires. Based on data both from NHSFS and CIEP our goal to calculate or assess the quantity of combusted waste was not possible to achieve, because we had no data of fire dimensions except for surface. We lacked the height of the burned objects. According to Bihałowicz et al. [8] the assumptions for height of incinerated waste ranged from 0.5 to 3.0 m. Therefore we calculated low and high variant of incinerated waste volume. Additionally for each for each type of waste, we considered the potential use, if it had not been incinerated in a fire.

3 Results and discussion

According to the data provided by NHSFS 243 waste fires occurred in 2018, and 176 in 2019. In the analysed years, an increase in the number of fires in the spring and summer period is observed. The number of fires in individual months is presented in fig. 1

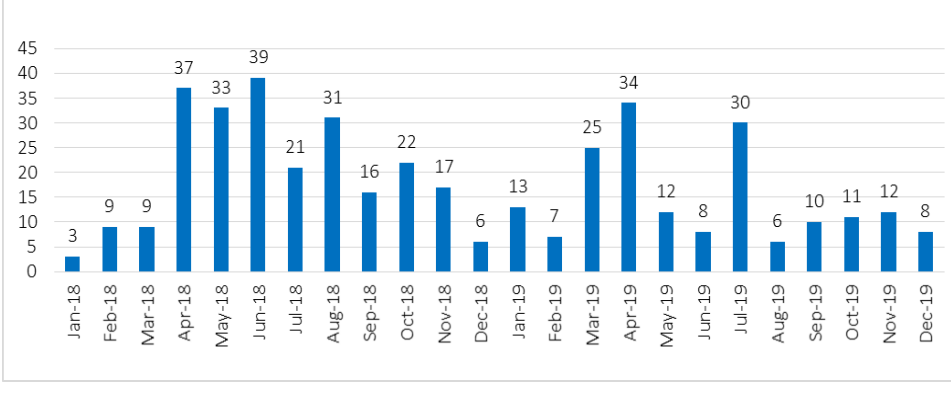

Fig. 1. Number of waste fires in individual months in 2018-2019.

The number of waste fires classified to size categories in 2018 and 2019 is in fig 2. Most often the fires were classified as small. In 2018, the most fires took place in the Łódź province (45), Lower Silesia (29) and Silesia (28). In 2019 in the Silesia (30), Lower Silesia (17) and Holy Cross province (16). Silesia is the most industrialised region in Poland and at the same time the most densely populated with large number of waste facilities.

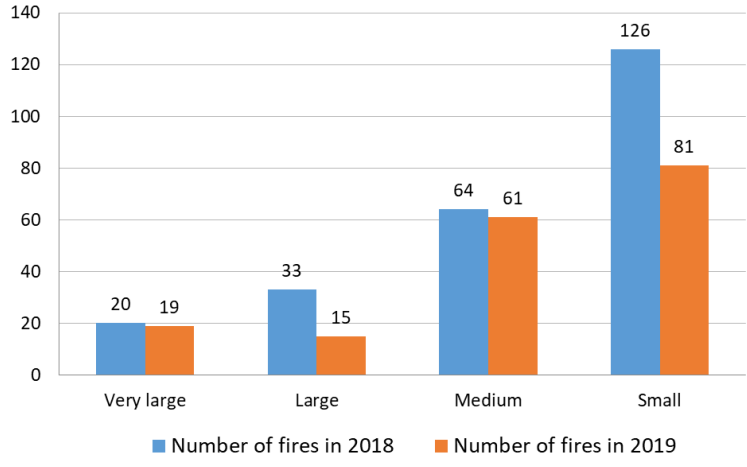

Fig. 2. Number and size of waste fires in Poland in 2018 and 2019

There were 20 very large fires in 2018 and 19 in 2019 and accordingly 33 large fires in 2018 and 15 in 2019. The location of very large and large waste fires is shown in fig. 3. In 2018 the largest fires (above 5000 m^2) took place in: Jakubów (Masovian province) – storage site of hazardous waste; Radom (Masovian province) – landfill site with MBT post-processed waste; Żory (Silesian) – waste treatment facility with old tires; Studzianki (Podlaskie province) – mixed municipal waste, waste treatment facility; Dąbrówka Wielkopolska (Lubuskie) – plastics, storage site; Grabów (Łodź province) - plastics, storage site; Wrocław (Lower Silesia) – plastics, waste treatment facility.

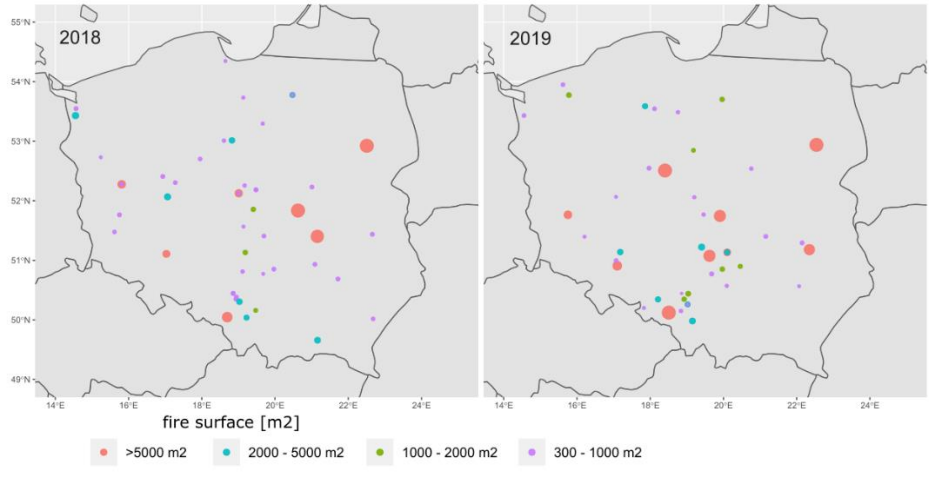

Fig. 3. Location of large and very large waste fires in Poland in 2018 and 2019

In 2019 the biggest fires above 5000 m^2 were following: Gać (Lower Silesia) – bulky and MBT post-processed waste, waste treatment facility; Jastrzębie – Zdrój – landfill; Fałków (Holy Cross province) – plastics and textiles, waste treatment facility; Serniki (Lublin province) – old tires, waste treatment facility; and the fires above 3000 m^2: Pysząca (Greater Poland) – plastics, waste treatment facility, Studzianki (Podlaskie) - mixed municipal waste –waste treatment facility; Ruszczyn (Łodź province) – landfill.

The total fire surface for large and very large fires in 2018 and 2019, for each type of waste, is shown in table 2. The waste which combusted in the greatest areas were: plastics and post-processed waste from MBT installations, including Refuse Derived Fuel (RDF), but also municipal unprocessed waste. Differences between values in 2018 and 2019 are due to different methods of data administration. In 2018 plastics and textiles were considered together, in 2019 textiles were listed separately. In 2018 more municipal waste was combusted comparing to 2019. On the other hand in 2019 CIEP did not specify waste type for many sites. After careful analysis of data by the NHSFS we classified that waste as municipal. But first of all many more fires occurred in 2018 than in 2019. Altogether waste fires in 2018 covered area of 169440 m^2 (16,94 ha), not counting small and medium fires, and in 2019 - 68352 m^2 (6,83 ha).

Table 2. Types of burned waste and the total fire surface for large and very large fires.

Burned waste type	**Total surface of fires [m^2] in 2018 and 2019**	
	2018	**2019**
MBT post-processed waste and RDF	30600	1018
No data*	8040	22119
biowaste		650
chemicals	800	
old paper	900	
municipal	20725	6700
hazardous waste	34100	
industrial waste	2300	1000
old tires	2819	5300
end-of-life vehicles	1300	
plastics	58656	16375
textiles		3490
bulky waste	8400	10500
waste electronic and electric equipment	800	1200
Total	**169440**	**68352**

* No data according to CIEP, based on the data by NHSFS we assumed waste to be municipal

Wastes that burned in fires are characterised by high calorific value and had potential as fuel or as a material to produce fuel. Some wastes could have been recycled into valuable secondary raw materials. The potential use of wastes that had been combusted is presented in the table 3. Additionally volume of combusted waste has been calculated in low and high variant and shown in table 3.

Taking into account only large and very large fires 170 thousand m^3 up to 1 million m^3 of waste burned in fires in 2018 and respectively 68 thousand m^3 up to 410 thousand m^3 in 2019. The exact calculation of combusted waste volume is not possible due to lack of data from NHSFS.. Therefore, the real volume of combusted waste is somewhere between low and high variant.

Table 3. Potential use and estimated volume of burned waste in 2018 and 2019 in low and high variants.

Burned waste type	Potential use of waste	Estimated volume of waste burned [m^3] in 2018 and 2019			
		2018		2019	
		Low variant	High variant	Low variant	High variant
MBT post-processed waste and RDF	RDF (fuel)	15300	91800	509	3054
biowaste	to be processed into RDF			325	1950
chemicals	recovery	400	2400		
old paper	recycling	450	2700		
municipal	to be processed into RDF	14383	86295	14410	86457
hazardous waste	recovery/ disposal	17050	102300		
industrial waste	recovery/ disposal	1150	6900	500	3000
old tires	RDF	1410	8457	2650	15900
end of life vehicles	recycling	650	3900		
plastics	recycling	29328	175968	8188	49125
textiles	RDF			1745	10470
bulky waste	RDF	4200	25200	5250	31500
waste electronic and electric equipment	recycling	400	2400	600	3600
Total volume		169440	1016640	68352	410112

4 Conclusions

1. Waste fires do not only cause air pollution and negative environmental impact, but also significant amounts of materials, which could had been recycled or recovered into energy, are wasted. Most often, plastics were burned (recycling potential) and municipal waste, processed and unprocessed - potential for use as fuel. The waste fires directly affect the depletion of natural resources, because with losses of secondary materials in fire, virgin materials are needed to produce plastics or fuel.
2. In 2018, even 1 million m^3 could burn in fires, however the exact calculation of volume of burned waste is not possible, because the NHSFS do not have data on fire objects dimensions (length, width, height).
3. Further research are needed to estimate quantities of combusted waste in tones, which is not easy because density of waste is very variable. Consequently the calorific value lost in fires could be estimated.

References

[1] Statistics Poland. Environment 2020. Warsaw, 2020.
[2] European Commission Council Directive 1999/31/EC of 26 April 1999 on the landfill of waste (OJ L 182 16.7.1999 as amended).
[3] Directive 2008/98/EC of the European Parliament and of the Council of 19 November 2008 on waste and repealing certain Directives (OJ L 312/3, 22.11.2008 as amended).
[4] Act of 14 December 2012 on waste. Republic of Poland. (Journal of Laws of 2021, item 779, as amended).
[5] European Commission. Closing the loop - An EU action plan for the Circular Economy. COM(2015) 614 final. Brussels, 2.12.2015.
[6] Regulation of the Ministry of Economy of 16 July 2015 on accepting waste for landfilling. Republic of Poland. (Journal of Laws of 2015, item 1277).
[7] National Waste Management Plan 2022. Republic of Poland. Resolution No 88 of the Council of Ministers of 1 July 2016 (item 784).
[8] Bihałowicz J.S., Rogula-Kozłowska W, Krasuski A. Contribution of landfill fires to air pollution - An assessment methodology. Waste Management 2021;125;182-91; DOI: 10.1016/j.wasman.2021.02.046.
[9] Nadal, M., Rovira, J., Díaz-Ferrero, J., Schuhmacher, M., Domingo, J. L. Human exposure to environmental pollutants after a tire landfill fire in Spain: Health risks. Environment international, 2016, V. 97, pp. 37-44. DOI: 10.1016/j.envint.2016.10.016.
[10] Downard, J. et al. 2015. Uncontrolled combustion of shredded tires in a landfill – Part 1: Characterization of gaseous and particulate emissions. Atmos. Environ. 104, 195–204. DOI: 10.1016/j.atmosenv.2014.12.059.
[11] Morales S.R.G.E., Toro A. R., Morales, L., Leiva G., M.A., 2018. Landfill fire and airborne aerosols in a large city: lessons learned and future needs. Air Qual. Atmos. Heal. 11, 111–121. DOI: 10.1007/s11869-017-0522-8.
[12] Statistics Poland. Environment 2018. Warsaw, 2018.
[13] Statistics Poland. Environment 2019. Warsaw, 2019.
[14] National Headquarters of the State Fire Service. Principles of recording events in the support system for the State Fire Brigade. Warsaw, 2019.

HYDROTHERMAL CARBONIZATION CONVERTING SEWAGE SLUDGE INTO CARBONACEOUS BIOFUEL

Klaudia Czerwińska[1,*]; Małgorzata Wilk[1]; Maciej Śliz[1]

[1] AGH University of Science and Technology,Faculty of Metals Engineering and Industrial Computer Science, Mickiewicza Av. 30, 30-059 Krakow, Poland
* corresponding author: kczerwin@agh.edu.pl

Abstract. *Sewage sludge is a type of waste which can present many difficulties because it contains not only organic and inorganic compounds or bacteria, but also dangerous compounds, e. g. heavy metals, hormones, pharmaceuticals, or pathogens. One innovative method of sewage sludge utilization and its conversion into a potential energy source is hydrothermal carbonization. This is the process of converting wet biomass into bio-oil, biogas, or hydrocarbons. Since there is no requirement for prior drying, this process works extremely well on sewage sludge. The resulting solid product (hydrochar) is structurally similar to natural lignite. It has a similar chemical composition and type of chemical bonds. The main aim of this study is to determine the potential for the production of a high carbon content fuel from sewage sludge using the hydrothermal carbonization method. In this study unfermented sewage sludge was used. The hydrothermal carbonization process was performed at temperatures of 200 and 220 °C and at 2 h of residence time. The effect of the selected process parameters on the properties of the resulting hydrochar for energy application was investigated using advanced instrumental methods. The results indicated that this process compacts the energy contained in the waste. Hydrochar has a calorific value higher than raw sewage sludge. The results depicted better energy properties in hydrochar than in raw sewage sludge (improved chemical composition, higher fixed carbon content and fuel ratio). This suggests the hydrothermal carbonization process is an efficient way to produce biocarbon. Additionally, the heavy metal transformation from raw sewage sludge to hydrochar and postprocessing water will be assessed.*

Keywords: *Sewage sludge, biofuel, hydrothermal carbonization.*

1 Introduction

The amount of sewage sludge in Europe is increasing rapidly due to a growing population and regulations aimed at improving wastewater quality. Incorrect management or lack of management of this waste can result in adverse environmental effects [1]. Sewage sludge contains not only organic and inorganic compounds or bacteria, but also dangerous compounds, i.e. heavy metals, hormones, pharmaceuticals or pathogens [2–5].

The processing of sewage sludge is a very cumbersome process. This is due to the highly complex form of the waste and its content of various substances. This waste contains, among

others, a high amount of moisture, heavy metals, and nitrogen. It consists of solid particles of various sizes suspended in contaminated water. Particles are usually a mixture of organic substances (i.e., proteins, fats, carbohydrates, and oils), inorganic substances, and microorganisms [4].

Taking into account the environmental issues concerning sewage sludge, it is important to choose an adequate disposal method. The most common methods of sewage sludge disposal includes incineration, co-combustion with solid fuel, and other alternative methods such as gasification, pyrolysis, wet oxidation, plasma technologies or hydrothermal carbonization (HTC). Most of these methods require a significant amount of energy to dry the raw material. However, the HTC process is an exception, as it is carried out in an aqueous environment, which allows the high-energy drying process to be omitted [6–8].

Hydrothermal carbonization is the process of converting wet biomass into bio-oil, biogas or hydrochar [9]. The hydrothermal process can be used to treat both inorganic and organic materials of various origins. Due to the lack of requirement for prior drying, this process is especially suitable for wet waste, e.g.: agricultural residue, forest biomass, industrial and municipal waste [10]. The presence of water in this process plays many significant roles such as solvent, catalyst, reactant or catalyst precursor [11]. Further, this process leads to densification of the energy contained in the material and also improves dewatering [12]. Disadvantages include the special attention required for the adequate treatment of the liquid phase.

Hydrothermal conditioning of sewage sludge is most often carried out in an aqueous environment with a temperature range of 180-250°C and autogenous pressure. These conditions lead to substrate decarboxylation, dehydration, and a reduction in hydrogen and oxygen [5,6,8,9]. During the HTC process several simultaneous reactions occur mainly hydrolysis, dehydration, decarboxylation, polymerization and carbonization [5].

The separated and dried solid HTC product, hydrochar, has a structure comparable to natural lignite, with a calorific value closely related to its carbon content [7]. It has a similar chemical composition and type of chemical bonds [8,10]. Different feedstock compositions do not cause significant structural changes in the hydrochar and, in fact, show morphological similarities [13]. From another point of view, the properties of sewage sludge can affect the hydrochar yield [9].

Herein, the study is focused on the fuel properties of hydrochar investigated under air condition by thermal analysis. Moreover, the structural and morphological changes are discussed through the use of scanning electron microscopy supported by energy dispersive spectroscopy of dried sewage sludge, hydrochars and their ashes.

2 Material and methods

2.1 Material

Dewatered sewage sludge was collected from an open digestion chamber at the municipal wastewater plant in Lubin in the Lower Silesia region of Poland. The raw sewage sludge contained more than 80% moisture and was stored at 4 °C to avoid the biodegradable process. The raw sewage sludge sample was dried and prepared for further analyses.

2.2 Hydrothermal conditioning procedure

Prior to the experiments the raw material was diluted in distilled water in an adequate quantity to ensure easy stirring and then the solution was placed in the reactor chamber, namely, a 1000 ml steel Zipperclave Stirred Reactor. Next, the reactor was heated up to 200 °C or to 220 °C, and when the temperature was reached, the solution was maintained therein for a strictly defined time - 2 h. Then, the reactor was cooled down and the solution was evacuated and separated by a filtration apparatus to obtain a wet solid material and liquid-filtrate. The solid material was dried and placed in an airtight container for further analyses.

2.3 Proximate and ultimate analyses

The ash, volatile matter and moisture contents were determined for dried sewage sludge and hydrochars in accordance with the European standards: PN-EN ISO 18134-1:2015-11, EN 15403:2011, EN 15402:2011. Ultimate analysis (carbon, hydrogen, and nitrogen content) was performed on Truespec CHNS Leco Elemental Analyzer (CHNS628) according to PKN-ISO/TS 12902:2007 standard.

2.4. Higher Heating Value

The HHV was determined using a Leco AC500 calorimeter equipped with a calorimetric bomb. The combustion of the hydrochar was carried out in an oxygen atmosphere to ensure complete combustion of the sample. The sample, in a crucible in the form of a compressed tablet, was placed in a combustion chamber. Then, the bomb was filled up with oxygen and placed in a calorimetric vessel containing water, where the wire was plugged in to ignite the material. The sample was combusted, and the temperature of the water was calculated. At the end of the combustion process the HHV was determined based on the recorded temperature with reference to the initial mass of the tested sample.

2.5 SEM

Scanning electron microscopy, by energy dispersive spectroscopy, was employed to determine changes in the structure and surface of the dried sewage sludge, hydrochars. Analysis was performed by an FEI Inspect S50 microscope using a low vacuum with backscattered electrons.

2.6. Combustion profiles of the samples

Thermogravimetric analysis was carried out on the solid materials to determine the effect of temperature on the carbonization process. The samples were heated to the desired temperature at a constant rate in an air environment. The following parameters were recorded: mass loss of the sample, temperature, and thermal effects. The results were presented in the form of TG, DTG, and DSC curves, respectively. Thermogravimetry (TG) showed the mass loss of the samples in comparison to the initial mass. Differential thermogravimetry (DTG) showed the rate of mass loss over time. Differential scanning calorimetry (DSC) determined the thermal (endothermic and exothermic) effects. Based on these data, the key combustion factors of the solid products were determined.

3 Results

The proximate and ultimate analyses, HHV, fuel and atomic ratios of dried sewage sludge and hydrochars are presented in Table 1.

Table 1. Properties of dried sewage sludge and hydrochars, db.

	FC [%]	sh [%]	M [%]	FC/VM	C [%]	H [%]	N [%]	S [%]	O [%]	O/C	H/C	HV [MJ/kg]
S	0.76	2.78	6.45	0.16	9.20	5.73	6.48	1.37	4.44	0.47	1.75	17.71
TC 200	2.21	6.58	1.21	0.24	41.20	5.16	3.90	1.00	2.16	0.22	1.50	19.04
TC 220	2.93	8.98	8.09	0.27	0.90	4.95	3.72	1.00	0.45	0.19	1.45	18.85

HTC - hydrochar; FC - fixed carbon; VM - volatile matter; C - carbon; H - hydrogen; N - nitrogen; S - sulphur; O – oxygen (calculated by difference); HHV - higher heating values

During the hydrothermal carbonization process, the percentage of fixed carbon (FC) increased. By comparing FC, as determined for hydrochars at two different temperatures of the HTC process, it can be concluded that as the temperature of the process increased, the fixed carbon also increased. The opposite trend was found for the ash contents. The lowest ash content was observed for dried sewage sludge, and the highest for the HTC process carried out at 220 °C. It was found that the higher the temperature of the process, the higher the ash content in the fuel. This was due to the rapid loss of volatile matter as the temperature rose. As a result, an increase in the fuel ratio (FC/VM), along with an increase in temperature, was observed.

The hydrothermal carbonization process affected the chemical composition of the samples. A slight increase in carbon content with a decrease in hydrogen, nitrogen, sulphur, and oxygen contents were found. The highest carbon value was found for HTC, performed at 200 °C, and resulted in the highest HHV value. A noticeable reduction in sulphur and nitrogen contents had a positive effect on the potential risk of harmful NOx and SO_x emissions.

Hydrothermal carbonization caused a decrease in the H/C and O/C atomic ratios for both hydrochars. The decrease in these values showed the positive effect of the hydrothermal carbonization process on hydrochar fuel properties.

The effect of the hydrothermal carbonization process on sewage sludge was also evaluated by SEM analysis. Figure 1 shows the SEM results. Initially, it was noticed that in dried sewage sludge the material particles were of different sizes and forms. However, after the hydrothermal carbonization process, a visible change occurred. The material was more homogeneous, and there was an increase in the number of smaller particles in the material after hydrothermal carbonization. This confirmed that, the higher the temperature, the smaller particles were observed. This was probably due to material degradation.

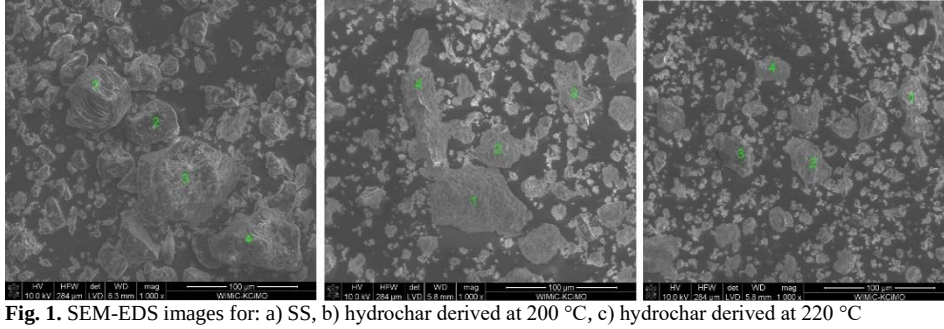

Fig. 1. SEM-EDS images for: a) SS, b) hydrochar derived at 200 °C, c) hydrochar derived at 220 °C

Hydrothermal carbonization had an influenced combustion process of sewage sludge. Based on the TGA analysis, the following combustion indexes have been determined: ignition temperature (T_i), burnout temperature (T_b), ignition index (D_i), burnout index (D_b), combustion index (S) and combustion stability index (H_f). These data are summarized in Table 2. By analyzing Table 2, it can be concluded that the hydrothermal carbonization process caused an increase in the ignition temperature but also a decrease in the combustion temperature of the samples. The ignition temperature for dried sewage sludge was 206 °C, while for the material after hydrothermal carbonization was 237 °C and 233 °C. The burnout temperature for dried sewage sludge was recorded at 547 °C and for the material after the HTC process, it decreased along with the temperature of the HTC process to 473 °C and 481 °C, respectively. The ignition index (D_i) illustrates the ease in which volatile matter was released from the fuel. However, a lower D_i signalled a problem with VM release in the early stage of combustion. The value of the D_i parameter for raw sewage sludge is the highest at 0.0062 ($\%\cdot min^{-3}$). For hydrochars, it was slightly lower a 0.0051 ($\%\cdot min^{-3}$) for HTC 200 °C and 0.0044 ($\%\cdot min^{-3}$) for HTC 220 °C.

The combustion index (S) mirrors the combustion, ignition, and burnout properties of the hydrochar. The highest value of this index was calculated for dried sewage sludge and resulted in $12.3\cdot10^{-8}$ ($\%\cdot min^{-2}\cdot°C^{-3}$). It was observed that as the temperature increased, the combustions index S decreased. For HTC 200 °C it was $9.5\cdot10^{-8}$ ($\%\cdot min^{-2}\cdot°C^{-3}$) and for HTC 220 °C it was $7.9\cdot10^{-8}$

(%·min^{-2}·°C^{-3}). The decrease of this parameter is related to the content of volatile matter in the material. The higher the volatile matter content was, the higher the combustions index was calculated. These conclusions were also confirmed by the properties of dried sewage sludge and hydrochars (Table 1).

The H_f index reflects the rate and intensity of combustion processes. As the H_f increases, combustion efficiency decreases. The lowest H_f index was determined for dried sewage sludge. The value of this parameter increased with an increase in the temperature of the HTC process and was recorded at 898.5 °C and 960 °C for HTC 200 °C for HTC 220 °C, respectively. An increase in the H_f parameter suggests a decrease in the intensity and rate of combustion in the material after the hydrothermal carbonization process.

Taking into account the analysis of the above parameters it was concluded that dried sewage sludge started to burn earlier and finished later and, as a consequence, the combustion process was longer in comparison to hydrochars. However, it is worth noting that after the HTC process, the energy contained in the sludge was significantly concentrated in comparison to dried sewage sludge due to a higher HHV content in hydrochars. Moreover, it should be underlined that the hydrothermal process significantly improved the dewatering of sewage sludge signifying that less energy is required to dry the pretreated sewage sludge to obtain more carbonaceous material. Furthermore, it is interesting to note that the HTC process took place at temperatures that are sufficient for removing microorganisms from sewage sludge and limiting biological processes. Also, solid fuel prepared in this way can be easily pelletized and stored

Table 2. Combustion parameters

	SS	HTC 200	HTC 220
T_i [°C]	206	237	233
t_i [min]	18.23	21,22	19.95
T_b [°C]	547	473	481
t_b [min]	52.25	44.93	45.70
$t_{0.5}$ [min]	17.65	18.40	18.65
t_1 [min]	24.52	26.89	28.18
T_1 [°C]	269	294.44	308
DTG_1 [%/min]	2.78	2.91	2.49
DTG_{mean} [%/min]	1.03	0.87	0.826
D_i [%·min^{-3}]	0.0062	0.0051	0.0044
D_b [%·min^{-4}]	12.3E-5	13.1E-5	10.4E-5
S [%·min^{-2}·°C^{-3}]	12.3E-8	9.5E-8	7.9E-8
H_f [°C]	764.3	898.5	960.0

DTG_{mean} – mean combustion rate; DTG_1 – maximum combustion rate;
$D_i = DTG_1 / (t_1 \cdot t_i)$, t_1 – corresponding time for DTG_1, t_i – ignition time;
$D_b = DTG_1 / (t_1 \cdot t_b \cdot t_{0.5})$, t_b – burnout time, $t_{0.5}$ - time range of $DTG/DTG_1 = 0.5$;
$S = (DTG_1 \cdot DTG_{mean}) / (T_i^2 \cdot T_b)$;
$H_f = T_1 \cdot \ln(t_{0.5} / DTG_{mean})$

Table 3 summarized the results of the X-ray fluorescence analysis. In the case of oxides, the hydrothermal carbonization process resulted in a decrease in sodium oxide, potassium oxide, and phosphorus oxide, and an increase in magnesium oxide, aluminium oxide, calcium oxide, sulphur oxide, and iron oxide. The hydrothermal carbonization process also affected the heavy metal content of sludge. Increases were observed in the contents of lead, copper, and zinc compounds, whereas decreases in the contents of chromium and nickel compounds were evident.

Table 3. Results of XRF analysis.

Component	SS [%]	HTC 200 [%]	HTC 220 [%]
Na_2O	0.8153	0.5066	0.4567
MgO	4.6777	4.8100	4.9882
Al_2O_3	5.4761	6.4932	6.1576
SiO_2	20.4600	21.3478	19.9081
P_2O_5	29.5347	26.8832	26.9039
SO_3	2.5372	2.8503	2.9972
Cl	0.0404	0.0245	0.0211
K_2O	3.1679	1.4399	1.3127
CaO	20.026	21.1726	22.1495
Fe_2O_3	10.5483	11.3501	12.0205
ZnO	0.3586	0.4320	0.4288
PbO	0.0526	0.0631	0.0611
Cr_2O_3	0.0809	0.0808	0.0727
NiO	0.0163	0.0132	0.0160
CuO	0.1568	0.1943	0.1833

4 Conclusions

The effects of the hydrothermal carbonization process, conducted at two different temperatures, 200 and 220 °C, on sewage sludge were investigated. The temperature at 200 °C significantly improved the carbonaceous properties of the sludge by increasing the solid carbon content and, consequently, its calorific value. The ash content of hydrochar was higher than that of dried sewage sludge and increased along with an increase in the temperature of the hydrothermal process, whereas for volatile matter, the opposite trend was found. As a result, the fixed carbon increased with an increase in the temperature of the pretreatment process. In addition, SEM analysis confirmed that a higher process temperature had more profoundly affected the degradation of the material giving more homogeneous and fragmented particles. Based on TG, DTG, and DSC data, the combustion profiles and indexes were determined indicating that dried sewage sludge combusted for longer and probably in a more violent and unstable way than hydrochars due to the high volatile matter content and high heat loss.

References

[1] Parshetti GK, Liu Z, Jain A, Srinivasan MP, Balasubramanian R. Hydrothermal carbonization of sewage sludge for energy production with coal. Fuel 2013;111:201–10. DOI: 10.1016/j.fuel.2013.04.052.

[2] Zhai Y, Liu X, Zhu Y, Peng C, Wang T, Zhu L, et al. Hydrothermal carbonization of sewage sludge: The effect of feed-water pH on fate and risk of heavy metals in hydrochars. Bioresour Technol 2016;218:183–8. DOI: 10.1016/j.biortech.2016.06.085.

[3] He C, Wang K, Giannis A, Yang Y, Wang JY. Products evolution during hydrothermal conversion of dewatered sewage sludge in sub- and near-critical water: Effects of reaction conditions and calcium oxide additive. Int J Hydrogen Energy 2015;40:5776–87. DOI: 10.1016/j.ijhydene.2015.03.006.

[4] Syed-Hassan SSA, Wang Y, Hu S, Su S, Xiang J. Thermochemical processing of sewage sludge to energy and fuel: Fundamentals, challenges and considerations. Renew Sustain Energy Rev 2017;80:888–913. DOI: 10.1016/j.rser.2017.05.262.

[5] Wang L, Chang Y, Li A. Hydrothermal carbonization for energy-efficient processing of sewage sludge: A review. Renew Sustain Energy Rev 2019;108:423–40. DOI: 10.1016/j.rser.2019.04.011.

[6] Wang T, Zhai Y, Zhu Y, Li C, Zeng G. A review of the hydrothermal carbonization of biomass waste for hydrochar formation: Process conditions, fundamentals, and physicochemical properties. Renew Sustain Energy Rev 2018;90:223–47. DOI: 10.1016/j.rser.2018.03.071.

[7] Kim D, Lee K, Park KY. Hydrothermal carbonization of anaerobically digested sludge for solid fuel production and energy recovery. Fuel 2014;130:120–5. DOI: 10.1016/j.fuel.2014.04.030.

[8] Aragón-Briceño CI, Grasham O, Ross AB, Dupont V, Camargo-Valero MA. Hydrothermal carbonization of sewage digestate at wastewater treatment works: Influence of solid loading on characteristics of hydrochar, process water and plant energetics. Renew Energy 2020;157:959–73. DOI: 10.1016/j.renene.2020.05.021.

[9] Azzaz AA, Khiari B, Jellali S, Ghimbeu CM, Jeguirim M. Hydrochars production, characterization and application for wastewater treatment: A review. Renew Sustain Energy Rev 2020;127. DOI: 10.1016/j.rser.2020.109882.

[10] Zhao P, Shen Y, Ge S, Chen Z, Yoshikawa K. Clean solid biofuel production from high moisture content waste biomass employing hydrothermal treatment. Appl Energy 2014;131:345–67. DOI: 10.1016/j.apenergy.2014.06.038.

[11] Mäkelä M, Fraikin L, Léonard A, Benavente V, Fullana A. Predicting the drying properties of sludge based on hydrothermal treatment under subcritical conditions. Water Res 2016;91:11–8. DOI: 10.1016/j.watres.2015.12.043.

[12] Zhao P, Shen Y, Ge S, Yoshikawa K. Energy recycling from sewage sludge by producing solid biofuel with hydrothermal carbonization. Energy Convers Manag 2014;78:815–21. DOI: 10.1016/j.enconman.2013.11.026.

[13] Alatalo SM, Repo E, Mäkilä E, Salonen J, Vakkilainen E, Sillanpää M. Adsorption behavior of hydrothermally treated municipal sludge & pulp and paper industry sludge. Bioresour Technol 2013;147:71–6. DOI: 10.1016/j.biortech.2013.08.034.

TECHNICAL AND ECONOMIC ASSESSMENT OF SELECTED HEATING SYSTEMS FOR A SINGLE-FAMILY BUILDING BASED ON LCC (LIFE CYCLE COST)

Paulina Zielinko[1,*]; Dorota Anna Krawczyk[1,2]

[1] Bialystok University of Technology, Faculty of Civil Engineering and Environmental Sciences, Bialystok, Poland
[2] Department of HVAC Engineering, Bialystok, Poland
* corresponding author: paulina.zielinko@gmail.com

Abstract. *The article presents a technical and economic analysis of the use of the most popular renewable energy systems for heating and preparing domestic hot water for a selected free-standing building residential. The analysis was carried out for selected variants of heating systems and compared with the selected ones conventional heat sources. For each of the systems, the investment and operating costs were determined and costs incurred over the entire life cycle of the product. The basic criterion for selecting a specific system heating is an economic bill. Based on the detailed energy characteristics of the analysed facility, the main parameters for the selection of the assumed heat sources were determined. At work the LCC (Life Cycle Cost) method was used. This method allows you to determine the estimated, total investment and operating costs of the system in the adopted cycle of its life.*

Keywords: *technical and economic analysis, renewable energy systems, Life Cycle Cost*.

1 Introduction

The increase in the share of renewable fuels in the energy balance has recently become a key issue in the global economy. It is related to a large extent with a rapidly declining stock of traditional fuels and progressive degradation of the natural environment.
One of the solutions improving the energy efficiency of buildings, with particular emphasis on individual households in terms of space heating, is the promotion of installations in which heat is produced by heat pumps. These devices work by absorbing the ambient energy from the air, water or soil, and then, using the vapor compression cycle, provide the building with heat at a higher temperature. Air, water or ground can be used as heat reservoirs, depending on the type of heat pump [1-3]. The Energy Efficiency Index (COP) [4] is defined as the ratio of the amount of heat produced by the device to the amount of work delivered to the propulsion device. The COP value depends mainly on the temperature of the heat source and its variability. Due to the insignificant temperature differences between the ground and the ambient air, ground heat exchangers are coupled with heat pumps in order to achieve higher COP values [5]. Other important factors

influencing the COP values are the type and temperature of the medium used in central heating installations, and additional functions performed by the device [3].

Doseva and Chakyrova [6] from Bulgaria considered three different parameters for the evaluation of the analyzed heat pump systems, i.e. life cycle costs (LCC), seasonal coefficient of performance (SCOP) and seasonal energy efficiency rate (SEER). On the basis of the conducted research, they noticed that the best results of the analyzed indicators are achieved when AWHP is designed for 50% of the building's heat demand.

Three Canadian scientists conducted an LCC analysis of four variants of renewable energy and heat pumps for three different types of homes located in the Toronto area. The analyzed combinations include a standard air source heat pump (ASHP), a ground source heat pump (GSHP), a cold climate air source heat pump (CC ASHP) and a solar assisted air source heat pump (SAHP). According to them, the best choice for buildings that are less efficient with higher heat load is the standard ASHP system (based on 20 year life cycle cost). GSHP system it becomes the better solution as the heating load is reduced. It was found that ground source heat pump systems are the most economically viable for a "Net Zero Ready" (NZR) newly constructed house. [7]

Although, the development of mining techniques postpones the moment when world resources become unavailable, nevertheless there is awareness of the occurrence of such a situation in the future. Postponement of the associated energy crisis with the depletion of fossil fuel resources can be achieved in two ways [8]:

- By increasing the share of renewable primary energy in the global energy balance.
- By reducing energy demand primary.

Taking into account the climatic conditions in Poland, several renewable energy sources (RES) can be used in single-family houses. These are: solar collectors to heat utility water, photovoltaic cells or a home wind farm generating electricity, biomass boilers or a heat pump used in the heating system, recuperators to recover energy from ventilation, waste heat recovery system, ground heat exchangers and the so-called hybrid solutions, combining various RES. Heat pumps [9] are enjoying more and more interest of the owners of single-family houses. Around 40% of investors are considering the possibility use of the heat pump in your own home. The national and international energy policy forces investors to include renewable energy systems in their newly built house designs. At the same time, there is a great awareness of relatively higher costs at the investment stage in the case of heating systems with the use of heat pumps, with relatively lower operating costs of these systems. In view of the constantly rising cost of carriers energy, the ability to perform a technical and economic analysis use of heat pumps in construction in relation to conventional ones heat sources is of great practical importance that it translates directly into the costs of thermal energy for heating and domestic hot water.

2 Methodology

The study uses the LCC (Life Cycle Cost) method [10], which allows to determine the estimated, total investment and operating costs of the system in the considered life cycle (1). It is based on a comparison of the investment outlays for the adopted solution of the heating system and preparation of domestic hot water for a residential building and the operating costs increasing with the passage of the system's useful life. A compressor air source heat pump and a gas condensing boiler were selected to analyse the two heating systems.

$$LCC = IC + \sum_{t=1}^{n} \frac{COF_t}{(1+s)^t} \; [zł] \tag{1}$$

where IC is the cost of purchasing and running the system in PLN, COF is the annual cost of using the system in PLN, n is the assumed number of years for the life cycle of the system (20 years), t is the next year of the "life" of the system, s is the real rate interest (discount).

Operating costs were calculated on the basis of the sum of unit costs in individual time intervals and servicing costs. The calculations were based on the number of heating hours in a

season, assuming about 200 days of heating season. The meteorological data were adopted for the city of Bialsytok with the hourly value of the temperature of the dry thermometer (DBT). Hourly electricity demand was assumed as the quotient of heat demand for final energy and COP generation efficiency. And the production efficiency was based on the manually calculated COP characteristic as a function of the temperature difference (for the given outside air temperature – Figure 1).

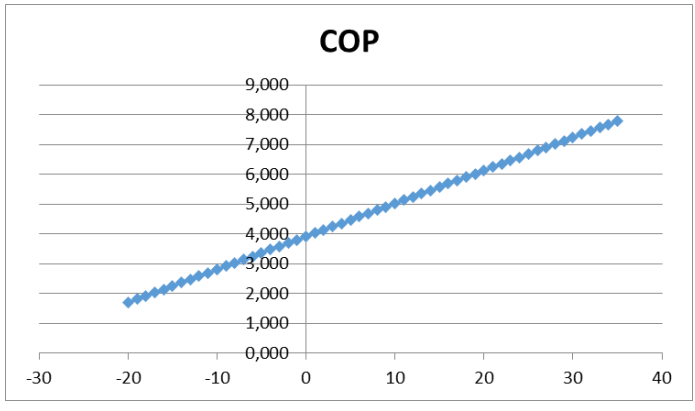

Fig. 1. COP characteristic as a function of temperature difference (calculated on the basis of the manufacturer's technical data).

3 Results

The assumption of the analysis was to conduct an assessment of the existing single-family building with designated energy indicators defining the building's demand for thermal energy for central heating and domestic hot water. The object under analysis is a one-story building with an attic located in the IV climate zone of Poland, near Bialystok. The annual heat demand of the facility according to the energy performance is 6265 kWh. An overview of the building's general data and the results for useful, final and primary energy are presented below (Table 1).

Tab. 1. Data from the energy performance of the building.

Data obtained on the basis of the energy performance of the newly built house	
Building area	202,43 m^2
Temperature-controlled area	217,57 m^2
Usable area	258,69 m^2
Building cubature	1125 m^3
Annual heat demand by the building	6265,69 kWh/year

The assumptions made for the analysis:

- Average outdoor temperature in an hourly cycle - based on data from stations from the Institute of Meteorology and Water Management.
- Air heat pump - PUMP VITOCAL 200-A air / water in monoblock version - AWO-M-E 201.A10 [4].

- Heating season - from 30 September to 1 May.
- Percentage share of heat in the season (hourly cycle) was calculated.

At an outside temperature of -10 degrees, the operation characteristics of the pump are as shown in Figure 2.

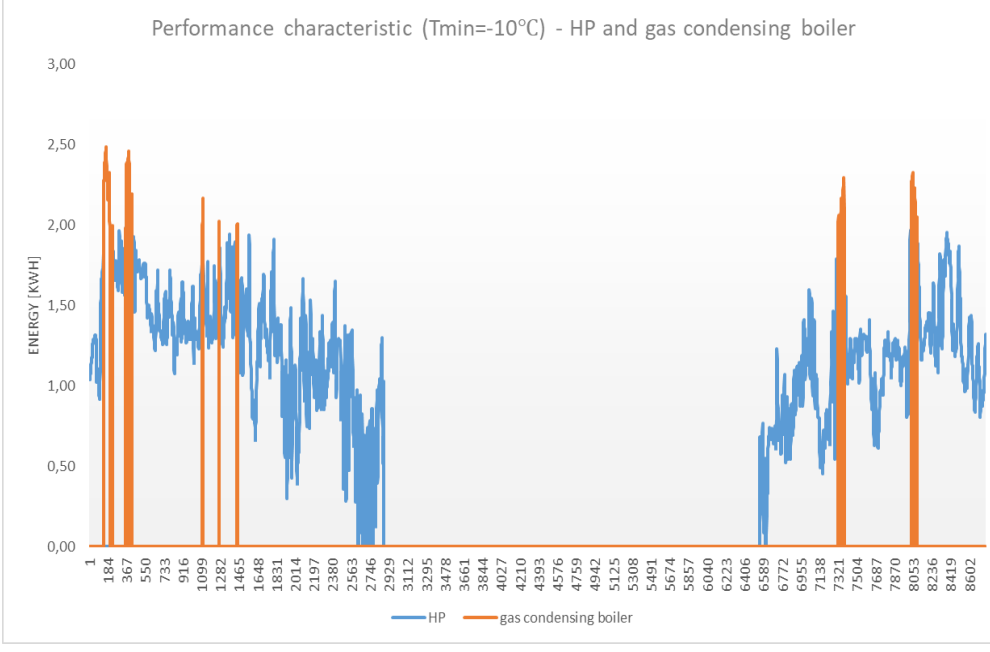

Fig. 2. Performance characteristics of individual systems for an outside temperature of -10°C.

The estimated values of the investment and operating expenditures of individual systems are presented in Figure 3-4. The expected life cycle of the system is 20 years.

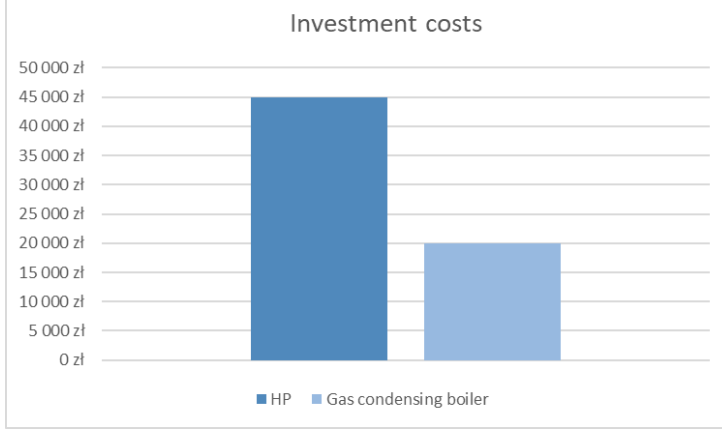

Fig. 3. Investment costs

The above figure shows that the investment cost of heating systems based on a heat pump is much higher than that based on a conventional source, but the situation changes in the next diagram, where the operating costs of the heat pump are less than half of the cost of the gas condensing boiler.

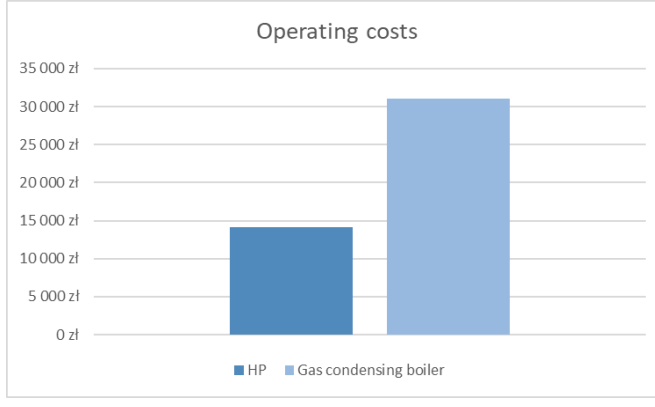

Fig. 4. Operating costs.

The annual demand for electricity (compressor coverage) for a system with a heat pump was determined by dividing the seasonal heat demand of the building by the production coefficient (COP) of the pump (Figure 5).

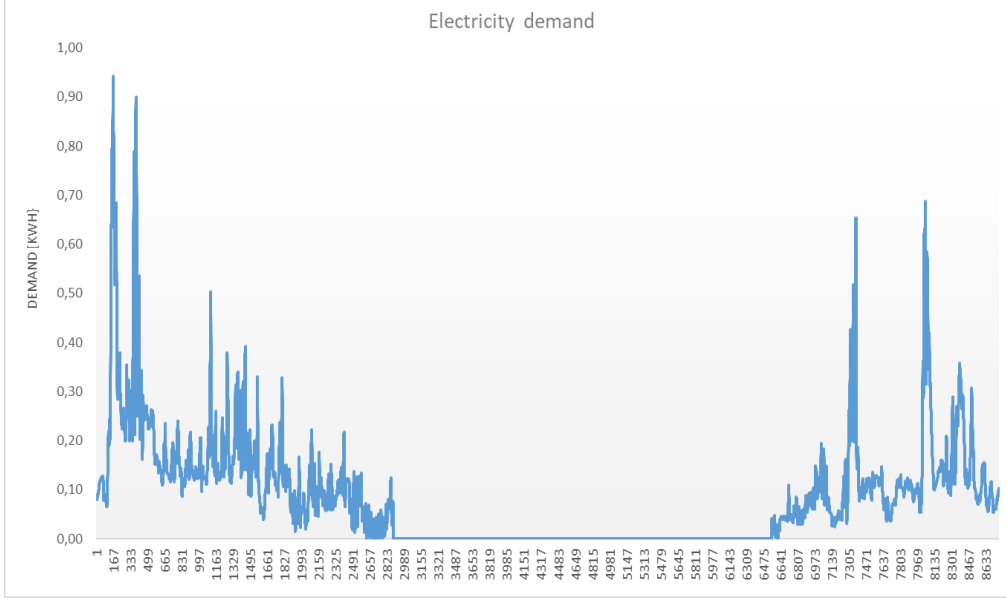

Fig. 5. Electricity demand (compressor operation).

The life cycle costing of the system depends largely on the real interest rate, which depends on the inflation rate and the nominal interest rate. Due to the difficulties in accurately forecasting the real discount rate, the LCC method was based on constant prices (Figure 6).

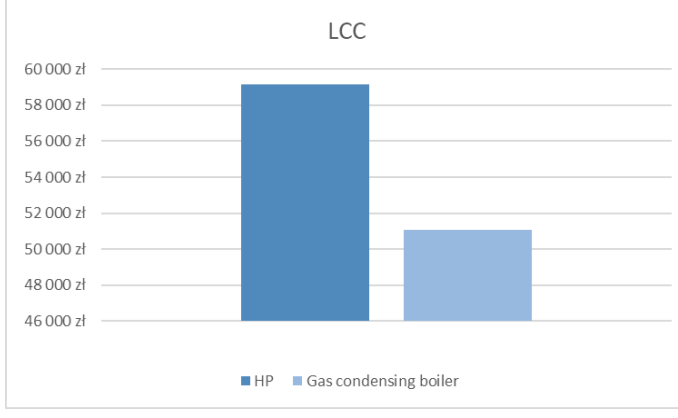

Fig. 6. Cost accounting.

The data analysis shows that the highest LCC value over 58 thousand PLN due to very high investment costs. For the remaining cases, the lowest values apply to a system based on a condensing boiler, here mainly the investment costs affect the low level of LCC.

4 Conclusions

Based on the economic analysis, it can be concluded that in the standard variant, the heat pump turns out to be more expensive than a gas condensing boiler, although the aspect of air cleanliness is not considered here, no additional costs at the construction stage related to the chimney, convenience of use (maintenance-free), lack of access to gas or changes / plans in regulations regarding the use of renewable energy sources. The barrier limiting the widespread use of heat pumps are high investment costs, but due to the depletion of traditional sources, they may become the primary source of energy in the future. Despite the relatively high investment costs of a heating system based on a compressor heat pump, this variant is able to compete with a system based on a gas condensing boiler in the case of purchasing electricity storage to cover the consumption for compressor operation.

References

[1] Saner, D., Juraske, R., Kübert, M., Blum, P., Hellweg, S., Bayer, P. Is it only CO2 that matters? A life cycle perspective on shallow geothermal systems. Renew. Sustain. Energy Rev. 2010, 14, 1798–1813.
[2] Bayer, P.; Saner, D.; Bolay, S.; Rybach, L.; Blum, P. Greenhouse gas emission savings of ground source heat pump systems in Europe: A review. Renew. Sustain. Energy Rev. 2012, 16, 1256–1267.
[3] Rubik, M. Refrigeration and Heat Pumps; Dom Wydawniczy MEDIUM Wydawnictwo: Warsaw, Poland, 2020.
[4] PN-EN 12831-1:2017-08, Energy Performance of Buildings—Method of Calculation of the Design Heat Load—Part 1: Space Heating Load, Module M3-3; The Polish Committee for Standardization: Warsaw, Poland, 2017

[5] Soltani, M.; Kashkooli, F.M.; Dehghani-Sanij, A.R.; Kazemi, A.R.; Bordbar, N.; Farshchi, M.J.; Elmi, M., Gharali, K., Dusseault, M.B. A comprehensive study of geothermal heating and cooling systems. Sustain. Cities Soc. 2019, 44, 793–818.

[6] Doseva N., Chakyrova D. Life cycle cost analysis of different residential heat pump systems. E3S Web of Conferences 207, 2020.

[7] Kegel M., Sunye R., Tamasauskas J. Life Cycle Cost Comparison and Optimisation of Different Heat Pump Systems in the Canadian Climate. Proceedings of eSim 2012: The Canadian Conference on Building Simulation, 2012.

[8] H. Rusak. Analiza lokalnych zasobów energii odnawialnej w kontekście zapotrzebowania na energię na przykładzie wybranych gmin, Polityka Energetyczna 2013, Tom 16, z. 3

[9] W. Marcinkowski. Pompy Ciepła. Wydawnictwo Budujemy Dom, 6/2008, 191-202.

[10] M. Świderski. Analiza LCC narzędziem wspomagającym ocenę projektów inwestycyjnych związanych z technika pompową. W: IX FORUM Użytkowników Pomp, Szczyrk 2003.

[11] https://www.viessmann.pl/

ARTIFICIAL NEURAL NETWORKS AND MACHINE LEARNING AS METHODS FOR IMPROVED AIR POLLUTION CONTROL

Katarzyna Szramowiat-Sala[1,*]

[1] AGH University of Science and Technology, Faculty of Energy and Fuels, Department of Coal Chemistry and Environmental Sciences, Mickiewicza Av. 30, 30-059 Krakow, Poland
* corresponding author: katarzyna.szramowiat@agh.edu.pl

Abstract. *Progress in science and technology is observed almost everywhere in the world, and currently most of new advanced technical solutions are mainly aimed at protecting human lives, protecting the environment and facing the ecological effects of industrial development. Recently, advanced methods have been sought to improve and predict the processes that are processed while exhausts are produced and pollutants are released to the atmosphere. Artificial intelligence (AI) is more interesting among researchers, especially since it has already found its interest in almost every area of technology. At the same time, it is continuously improved to fully replace a human in the near future in such activities, such as cooking, telemarketing, or driving a car. In this work, the application possibility of artificial intelligence (artificial neural networks – ANN) has been reviewed in some environmental aspects. On the basis of the reviewed papers, it was concluded that the artificial intelligence, using the proper computational algorithms and matrices, may be successfully applied in air pollution control systems for the forecasting of emitted pollutants depending on chosen factors.*

Keywords: *air pollution, control systems, artificial neural networks, machine learning, air quality improvement*

1 Introduction

Despite many programs aiming at improving air quality implemented almost in every country in the world, it may be expressed that these programs are not sufficient or that ecological awareness rises in human minds too slowly. On 31 October 2021 began the COP26 meeting in Glasgow where the United Nations discussed climate change which turned out to be the greatest risk facing the society. During the COP21 in Paris 2015 all countries agreed to work together to limit global warming to well below 2 degrees and aim for 1.5 degrees, to adapt to the impacts of a changing climate, and to make money available to deliver on these aims. Meanwhile, despite the great engagement of every country in programs aimed at improving air quality, they warned that they will probably not be able to meet the goal assigned in the Paris agreement until 2030. What could be the reason? And what steps should we take in our homes to support the world in changing air quality and changing life? Should governments change the strategy? Sustainable development seems to be the ideal balance between human health protection, avoiding environmental disasters, and necessary economic resources. Thus, there is probably one solution:

to provide more funds for structure programs aimed at improving the functioning of households without increasing fuel prices or with additional funds for fuel purchase. The more effective waste treatment and the broadening of education about environmental protection should also be developed. Every tiny step taken to avoid climate change is worth its weight in gold.

Artificial intelligence (AI) found its application in many areas including also environmental protection systems. Organisations like Google, Microsoft, or Tesla developed some "Earth Friendly" AI systems. For instance, Google implemented DeepMind (www.deepmind.com), which helped the organization to curb their data centre energy usage by 40 % making them more energy efficient and reducing overall GHG emissions. Installation of smart grids in cities can utilize artificial intelligence techniques to regulate and control parts of the neighbourhood power grid to deliver exactly the amount of electricity needed or requested from its dependents, against the use of conventional power grids that can be wasteful due to unplanned power distribution [1]. With AI-driven autonomous vehicles waiting to break into the automobile market, techniques like route optimization, eco-driving algorithms, and ride-sharing services would help in streamlining the carbon footprint and reducing the overall number of vehicles on the road [2].

Viewed on a macro scale, the emergence of smart buildings and the smart cities in which they are built can leverage built-in sensors to use energy efficiently, and buildings and roads will also be constructed from materials that work more intelligently. Taking a nod to natural patterns, material scientists and architects have developed innovative building materials from natural resources, such as bacteria bricks [3], cement that captures carbon dioxide [4], and cooling systems that use the wind and sun [5]. Solar power is increasingly present within cities and outside to supply larger urban areas. These are the first early steps toward sustainable infrastructure cutting costs and helping to make the world's population environmentally friendly.

This paper aims to provide a short review of the applications of artificial intelligence in air pollution control systems.

2 Artificial neural networks – the background

The basics of artificial intelligence may be read in the previous paper by Szramowiat-Sala et al., 2021 [6]. Artificial neural networks (ANN) are the most popular mechanism applied in air pollution control and forecasting systems. ANNs have been developed to mimic the functioning of a human neural system, which is perfectly designed to process the signals from the entire organism through the dendrites with a specific synaptic strength (weight) through axons to the brain. The input to the network is represented by the mathematical symbol „x". Each of these inputs is multiplied by a connection weight 'w'. These products are simply summed, fed through the transfer function 'f' to generate a result and an output. 'b' is an error that occurs during the learning process (Fig. 2) [7].

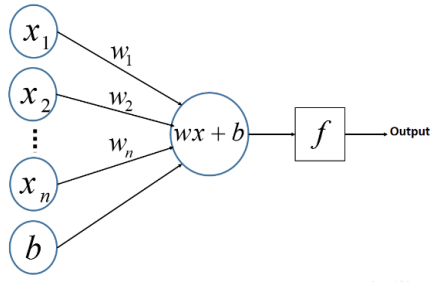

Fig. 1. The mathematical basis of artificial neural networks.

There are many examples of ANN architecture and computational or learning algorithms [8,9]. With the development of science and technology, these architectures and algorithms are also being developed. Fig. 3 shows the fully-connected feedforward backpropagation neural

networks. This means that each input is connected in each layer to the other. The full connections between the data sets implemented in the model are created. Another solution is to partition the data sets into subsets creating the acyclic networks. This allows optimizing the model and making the computational time shorter. Such operations are frequently used when neural networks are applied in forecasting of atmosphere pollution where many variables, like the concentration of many pollutants, and, on the other hand, the physical parameters like pressure, wind speed, temperature, humidity, solar radiation, etc. should be incorporated into the model algorithm [10–12]. Feedforward means that data sets go through each hidden layer. In acyclic networks, some data sets may „skip" a layer and move forward. While running the model, the inputs are provided and the outputs that are required to obtain, and the information which is loaded by a computational error is a result of computing. The backpropagation option allows to minimize this error until the ANN learns the training data [8].

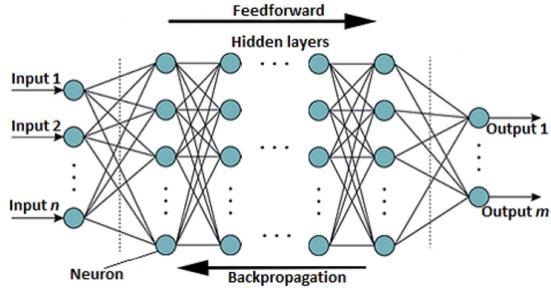

Fig. 2. A fully-connected feedforward backpropagation algorithm as an example of artificial neural networks.

3 ANN algorithms applied in air pollution control systems

Due to the fact that ANNs do not require an understanding and detailed knowledge of the processes that occur in the atmosphere or other environmental compartments, ANNs are a suitable alternative to commonly used computational models, such as real-time air quality forecasting models (RT-AQF) [10,13]. Models of this kind are sensitive to many factors, that is, the scale and quality of the parameters involved in the model, computationally expensive and dependent on large databases of several input parameters, of which some may not be available [14,15]. However, Russo et al., 2013 [12] advise to implement the models with an optimal amount of datasets. The minimization of data in the input layer improves the predictive power of ANNs. On the other site, according to Antanasijević et al., 2013 [16] the wide availability of the input parameters used in ANNs can overcome the lack of data and basic environmental indicators in many countries, which can prevent or seriously hinder the forecasting of particulate matter (PM) emission.

Perez and Reyes, 2006 [17] compared the application of neural networks reflecting the linear and non-linear models. In this work a three-layer feed neural network as a nonlinear model was applied, and a special neural network with no hidden layer as a linear model. Nonlinear models gave better results than linear models in forecasting of air pollution by PM10 from the perspective of 24 h. Antanasijević et al., 2013 [16] came up with similar conclusions. The ANN model has shown very good performance and demonstrated that the forecast of PM10 emission up to two years can be made successfully and accurately and were three times better than the predictions obtained from the conventional multilinear regression and principal component regression models that were trained and tested using the same datasets and input variables. The advantages of few predictors (the multilayer perceptron, radial basis function, Elman network, and support vector machine) combined in the ensemble were also presented by Siwek and Osowski, 2012 [18]. The important advantage of the proposed approach is that it does not require very exhaustive

information about air pollutant, reaction mechanisms, and meteorological pollutant sources, and that they have the ability of allowing nonlinear relationships between very different predictor variables.

Interesting results were obtained by applying both artificial intelligence and statistical methods commonly used for PM10 source allocation. Singh et al., 2013 [19] used principal component analysis (PCA) for the purposes of identifying PM10 sources and tree-based ensemble learning models (single decision tree, decision tree forest, decision tree boost) to predict urban air quality in urban area in India. The proposed ensemble models successfully predicted the ambient air quality of the city and, according to the authors, they can be used as effective tools for its management. In the paper by Feng et al., 2015 a novel hybrid model was presented combining air mass trajectory analysis and wavelength transformation to improve the artificial neural network forecast accuracy of daily average concentrations of PM2.5 two days in advance. As the respective pollutant predictors were used as input to a multilayer perceptron (MLP) type of back-propagation neural network. The significant advantage of this hybrid model was its ability to predict the high peaks of PM2.5 concentrations, which are considered very critical factors in air pollution forecasting systems.

The paper of Rutherford et al., 2021 [20] is very worth of concern while considering the application of hybrids of AI and advanced instrumental analytical techniques for the purpose of PM generated from combustion sources. The hybrid algorithm of excitation-emission matrix (EEM) fluorescence spectroscopy and machine learning was developed. To train this model, the PMF source apportionment technique was applied. The EEM-ML approach was successful and moderately successful in predicting vegetative burning and mobile sources. However, the PMF usage for model training did not resolve source categories that would likely be valuable on a global scale such as forest fires, various cookstove and home heating fuels (e.g., biomass, kerosene, LPG, and coal), or diesel versus gasoline exhaust. Using source apportionment data that resolved these sources to train an EEM-ML model could allow EEM-ML to apportion these important sources of PM pollution. This was partially achieved by Song et al., 2001 [15], who proposed multivariate calibration based on single particle mass spectral data to apportion the gasoline and diesel generated emissions.

The useful properties of artificial intelligence in air quality forecasting and in the development of cost-effective control strategies were also confirmed by other authors [17,22–25].

4 Conclusions

Atmosphere is a complex medium that consists, in addition to constant gaseous components such as N_2, O_2, and CO_2, of other chemicals that influence the quality of ambient air less or more. The atmosphere components undergo many physical and chemical transformations, which change dependently on the temperature, pressure, wind speed, solar radiation, or relative humidity. For this reason, the forecasting and prediction of air pollution is an enormous difficult challenge for both chemical, meteorologists, physicists, and modellers. The application of artificial neural networks which have been developed to mimic the processing of signals in human organism to the brain seem to be a promising tool applied in environmental protection and air quality control systems. The papers reviewed in this work proved this; however, the successful performance of the model applied depends on the topology of ANN or application of clusters with other computing mechanisms (statistical analysis, instrumental techniques).

Acknowledgements

Research project supported by the program 'Excellence initiative – research university' for the AGH University of Science and Technology. The authors also gratefully acknowledge the funding support given by AGH UST in Krakow within the subvention project no. 16.16.210.476.

References

[1] Fan D, Ren Y, Feng Q, Liu Y, Wang Z, Lin J. Restoration of smart grids: Current status, challenges, and opportunities. Renewable and Sustainable Energy Reviews 2021;143:110909. DOI: 10.1016/J.RSER.2021.110909.

[2] Ahmad T, Zhang D, Huang C, Zhang H, Dai N, Song Y, et al. Artificial intelligence in sustainable energy industry: Status Quo, challenges and opportunities. Journal of Cleaner Production 2021;289:125834. DOI: 10.1016/J.JCLEPRO.2021.125834.

[3] Gründling A, Collet JF. Editorial overview: "All in all, it is not just another brick in the wall": new concepts and mechanisms on how bacteria build their wall. Current Opinion in Microbiology 2021;62:110–3. DOI: 10.1016/J.MIB.2021.04.001.

[4] Zhan Q, Yu X, Pan Z, Qian C. Microbial-induced synthesis of calcite based on carbon dioxide capture and its cementing mechanism. Journal of Cleaner Production 2021;278:123398. DOI: 10.1016/J.JCLEPRO.2020.123398.

[5] Rykaczewski K. Rational design of sun and wind shaded evaporative cooling vests for enhanced personal cooling in hot and dry climates. Applied Thermal Engineering 2020;171:115122. DOI: 10.1016/J.APPLTHERMALENG.2020.115122.

[6] Szramowiat-Sala K, Osiecka-Drewniak N, Borovec K, Horak J, Golas J, Gorecki J. The possibilities of application of artificial intelligence in environmental monitoring systems. SDEWES, 2021.

[7] Zupan J, Gasteiger J. Neural networks: A new method for solving chemical problems or just a passing phase? Analytica Chimica Acta 1991;248:1–30.
DOI: 10.1016/S0003-2670(00)80865-X.

[8] Tadeusiewicz R. Introduction to neural networks. Kraków: 2021.

[9] Kaviani S, Sohn I. Application of complex systems topologies in artificial neural networks optimization: An overview. Expert Systems with Applications 2021;180:115073. DOI: 10.1016/J.ESWA.2021.115073.

[10] Zhang Y, Bocquet M, Mallet V, Seigneur C, Baklanov A. Real-time air quality forecasting, part I: History, techniques, and current status. Atmospheric Environment 2012;60:632–55. DOI: 10.1016/J.ATMOSENV.2012.06.031.

[11] Zhang Y, Bocquet M, Mallet V, Seigneur C, Baklanov A. Real-time air quality forecasting, part II: State of the science, current research needs, and future prospects. Atmospheric Environment 2012;60:656–76.
DOI: 10.1016/J.ATMOSENV.2012.02.041.

[12] Russo A, Raischel F, Lind PG. Air quality prediction using optimal neural networks with stochastic variables. Atmospheric Environment 2013;79:822–30.
DOI: 10.1016/J.ATMOSENV.2013.07.072.

[13] Zarra T, Galang MG, Ballesteros F, Belgiorno V, Naddeo V. Environmental odour management by artificial neural network – A review. Environment International 2019;133:105189. DOI: 10.1016/J.ENVINT.2019.105189.

[14] Dutot AL, Rynkiewicz J, Steiner FE, Rude J. A 24-h forecast of ozone peaks and exceedance levels using neural classifiers and weather predictions. Environmental Modelling & Software 2007;22:1261–9. DOI: 10.1016/J.ENVSOFT.2006.08.002.

[15] Cabaneros SM, Calautit JK, Hughes BR. A review of artificial neural network models for ambient air pollution prediction. Environmental Modelling and Software 2019;119:285–304. DOI: 10.1016/j.envsoft.2019.06.014.

[16] Antanasijević DZ, Pocajt V V., Povrenović DS, Ristić MD, Perić-Grujić AA. PM10 emission forecasting using artificial neural networks and genetic algorithm input variable optimization. Science of The Total Environment 2013;443:511–9.
DOI: /10.1016/J.SCITOTENV.2012.10.110.

[17] Perez P, Reyes J. An integrated neural network model for PM10 forecasting. Atmospheric Environment 2006;40:2845–51. DOI: 10.1016/J.ATMOSENV.2006.01.010.

[18] Siwek K, Osowski S. Improving the accuracy of prediction of PM10 pollution by the wavelet transformation and an ensemble of neural predictors. Engineering Applications of Artificial Intelligence 2012;25:1246–58. DOI: 10.1016/J.ENGAPPAI.2011.10.013.

[19] Singh KP, Gupta S, Rai P. Identifying pollution sources and predicting urban air quality using ensemble learning methods. Atmospheric Environment 2013;80:426–37. DOI: 10.1016/J.ATMOSENV.2013.08.023.

[20] Rutherford JW, Larson T V., Gould T, Seto E, Novosselov I V., Posner JD. Source apportionment of environmental combustion sources using excitation emission matrix fluorescence spectroscopy and machine learning. Atmospheric Environment 2021;259:118501. DOI: 10.1016/j.atmosenv.2021.118501.

[21] Song XH, Faber NM, Hopke PK, Suess DT, Prather KA, Schauer JJ, et al. Source apportionment of gasoline and diesel by multivariate calibration based on single particle mass spectral data. Analytica Chimica Acta 2001;446:327–41. DOI: 10.1016/S0003-2670(01)01270-3.

[22] De Gennaro G, Trizio L, Di Gilio A, Pey J, Pérez N, Cusack M, et al. Neural network model for the prediction of PM10 daily concentrations in two sites in the Western Mediterranean. Science of The Total Environment 2013;463–464:875–83. DOI: 10.1016/J.SCITOTENV.2013.06.093.

[23] Donnelly A, Misstear B, Broderick B. Real time air quality forecasting using integrated parametric and non-parametric regression techniques. Atmospheric Environment 2015;103:53–65. DOI: 10.1016/J.ATMOSENV.2014.12.011.

[24] Fernando HJS, Mammarella MC, Grandoni G, Fedele P, Di Marco R, Dimitrova R, et al. Forecasting PM10 in metropolitan areas: Efficacy of neural networks. Environmental Pollution 2012;163:62–7. DOI: 10.1016/J.ENVPOL.2011.12.018.

[25] Grivas G, Chaloulakou A. Artificial neural network models for prediction of PM10 hourly concentrations, in the Greater Area of Athens, Greece. Atmospheric Environment 2006;40:1216–29. DOI: 10.1016/J.ATMOSENV.2005.10.036.

THE APPLICATION OF MODERN MATERIALS WITH SORPTION AND CATALYTIC PROPERTIES FOR MICRO-CONTAMINANTS REMOVAL

Wiktor Pacura[1,*]; Katarzyna Szramowiat-Sala[1]; Janusz Gołaś[1]

[1] AGH University of Science and Technology, Faculty of Energy and Fuels, Department of Coal Chemistry and Environmental Sciences, Mickiewicza Av. 30, 30-059 Krakow, Poland
* corresponding author: katarzyna.szramowiat@agh.edu.pl

Abstract. *In the today's world, air quality is one of the top priorities in environmental protection research and legislation. The BAT conclusions, EURO Emission Standards or recent EU Fit For 55 program implement severe restrictions in case of the exhaust gasses emissions. Besides main pollutants such as solid particles or various oxides, the exhaust gasses from stationary and mobile sources contain micro-contaminants (MCs), which are present in the exhaust in relatively low concentration. Due to the immense volume of the exhaust gases produced every day, even seemingly insignificant amounts of the MCs are a serious concern. The increasing prices of the platinum group metals such as Pt, Pd and Rh commonly used in exhaust aftertreatment systems compel researchers to focus on alternative materials. There are several conditions that these materials should meet (fulfil), i.e. sufficient thermal resistance. Studies show that the use of metals such as Cu, Co, Fe, Ni, or Mn improves oxidation of PAHs and their derivatives, thus it might be a valid solution for the MCs emission control. The aim of this work is to review the possibilities of the application of new materials with sorption and catalytic properties for the removal of MCs generated in combustion processes.*

Keywords: *micro-contaminants, exhaust, emission control, PAHs derivatives, PAHs, PGMs.*

1 Introduction

For many decades, the quality of air pollution has been a major concern of scientists and legislators. Numerous acts and laws have been implemented to improve or at least maintain air quality and prevent further deterioration. In the heavy industry and the commercial sector, the Best Available Techniques (BAT) regulations were implemented to use the best possible technologies to perform processes and manage waste. In Poland, air quality is regulated by the Ordinance of the Minister of the Environment [1] which limits the major pollutants, as can be seen in Table 1. The table lists most of the pollutants that are regulated, such as nitrogen oxides, sulphur dioxide, benzene, particulate matter (PM), etc. with yearly average limits; however, the ordinance also contains more precise limits with daily or hourly restrictions. There is also a trend to exclude all industry from the city borders and implement local regulations that are even more restrictive than the above-mentioned act.

Table 1. Levels of certain substances in the air

Pollutant	Benzene	NO_2	NO_x	SO_2	Lead	PM 2.5	PM 10	CO
Allowed concentration	5	40	30	20	0.5	20	40	10 000
Unit	$\mu g/m^3$							
Period	Calendar year							8 h.

In the case of the city of Krakow, the air quality improvement program prohibits the use of solid fuels in households in the city area. The smaller cities and villages are following this trend, therefore, the act is implemented in the whole voivodeship. One of remaining sources of the pollution in Krakow is vehicular emission. The quality of car exhaust is regulated by the Euro emission standards, which are implemented throughout the EU. The standard, similar to air quality acts, limits only the main pollutants, such as carbon oxides or nitrogen oxides. In 2017, the implementation of the Euro 6 standard began, introducing major changes such as a revised vehicle testing procedure or a particulate number (PN). Currently, the Euro 7 emission standard is under deliberation. Besides the more strict limits, one of the major proposals is implementation of some micro-contaminants (MCs) into the standards. In case of carbon dioxide, the relatively new Fit for 55 proposal aims to reduce CO_2 and ultimately achieve carbon neutrality. For vehicles, the program plans to reduce CO_2 emissions from the newly produced car fleet by 55% in 2030 and 100% in 2035. Table 2 compares the acts and proposals mentioned.

Table 2. Vehicle exhaust pollutants limits

Compound	CO	HC	NMHC	NO_x	HC+NO_X	M	N^*	O_2^{**}	C
	[g/km]						[#/km]	[g/km]	
Euro 1	3.16	–	–	–	1.13	–	–	–	–
Euro 5a	1.0	0.10	0.068	0.060	–	0.005			–
Euro 6d	1.0	0.10	0.068	0.060			$6 \cdot 1011$		–
Euro 7 (draft)	1.0	?		0.030 0.010	?	?	$1 \cdot 10^{11}$ $6 \cdot 10^{10}$	?	Some
Fit for 55 (2030)	–	–	–	–	–	–	–	55% cut***	–
Fit for 55 (2035)	–	–	–	–	–	–	–	100% cut***	–

*Gasoline Direct Injection only

**Average emission of the fleet

***Compared to the 2021 limits

In addition to the major pollutants, the exhaust of any source contains seemingly low quantities of MCs. However, the vast amounts of flue gases produced every day cause the MCs to add up to enormous quantities.

2 Micro-contaminants

In addition to gaseous compounds such as sulphur oxides and nitrogen oxides, the flue gas also contains solid particles described by mass and number. These indicators are presented in various acts and programs mentioned above. However, the mass or number itself cannot provide sufficient information on the toxicity of the exhausts. Solid particles contain a wide range of MCs such as polycyclic aromatic hydrocarbons (PAHs) or their nitric and oxygenated derivatives, metals, metalloids, or salts. A more accurate description of the risk of PM hazard to health and the environment can be achieved by using the toxic equivalency factor (TEF) [2]. The TEF

describes the toxicity of the specific component compared to the reference compound, benzo[a]pyrene, represent with TEF factor 1. Table 3. shows few TEF factors for the selected compounds. Dibenzo[a,h]anthracene has the same negative impact as benzo[a]pyrene. PAHs such as acenaphthene, fluorine, or pyrene have a TEF equal to 0.001, but their nitric derivatives have ten to hundred times more negative influence. The nitric derivative of chrysene, 6-nitrochyrsene, has TEF 10, which means that 1 g of this compound is as harmful as 10 g of benzo[a]pyrene.

Table 3. The TEF factor of selected compounds [2]

Compound	TEF	Compound	TEF
Benzo[a]pyrene	1	Dibenzo[a,h]anthracene	1
Naphthalene	0.001	Benzo[k]fluoranthene	0.1
Acenaphthene	0.001	5-Nitroacenaphthene	0.03
Fluorene	0.001	2-Nitrofluorene	0.01
Pyrene	0.001	1-Nitropyrene	0.1
Chrysene	0.01	6-Nitrochrysene	10

In addition to carbon-based components of exhaust fumes, inorganic compounds or elements are also present [3]. They are part of the mass and number of solid particles emitted from combustion processes. In industry, for example, in the coal plant, they originate from the fuel impurities or catalyst used during the process. According to previous Authors' studies of vehicle emission [4] inorganic matter in exhaust originates from fuel, engine oil, engine block and ambient air. In the case of fuel and engine oil, substances containing, for example, Na, Ca, K, or Zn are used as lubricant agents to improve the quality of combustion or act as a detergent to clean the surfaces of the engine. Inorganic MCs from the engine block, such as Al, Si, or Cu, originate from the wear of the engine. Finally, some of the MCs, e.g. containing barium, might be present in ambient air, used for combustion processes. They originate from road dust, tires, and brakes and travel through the air intake filter directly to the cylinder [4].

3 Micro-contaminants removal

Actions can be taken to reduce the impact of exhaust gases on the environment during every combustion step: before, during, and after. Actions before combustion include improving fuel quality. This can be achieved in various ways, for example, with a better and more thorough gasoline purification, decreasing the metal or sulphur content. In the case of solid fuels, the improvement can be obtained by using a better quality fuel that contains less water or halides or at least partially replacing the furnace charge. Another way to improve fuel is to use bioadditives such as bioethanol to reduce total CO_2 emissions, combustion-improving agents, detergents, etc.

During combustion, the most common type of emission control is the use of the catalyst, recirculation of exhaust gases, or the change of the timing and design of the engine architecture. The implementation of the catalyst can be expensive and generate an additional post-combustion product, such as ash or slag. In the case of solid fuel-powered furnaces, for example, in the coal plant, the flue gas recirculation can be introduced into the process during the solid particle removal, bypassing the stream of exhaust from the cyclone. In the case of the vehicle exhaust gas recirculation system, changing the engine architecture or various times, such as injection and fuel ignition times, etc. can also lead to a decrease in pollutant emission, but the change can be too insignificant to justify the enormous cost associated with the design changes.

Finally, exhaust aftertreatment is responsible for decreasing the concentration of sulphur oxides, nitrogen oxides or particulate matter. It can be achieved with the use of scrubbers, particulate filters, or a dedicated catalyst.

The studies indicate that the addition of oxygenated compounds is responsible for the emergence of non-regulated emission. The addition of ethanol to gasoline increases the emission of monocarboxylic acids [5], dicarboxylic acids [6], formaldehyde and acetaldehyde [4]. Other

changes, such as adding better fuel or changes during combustion, can be expensive and time-consuming with little effect on the emission. The changes in exhaust aftertreatment compared to other steps are inexpensive and relatively straightforward to implement.

4 Materials for the removal of the micro-contaminants

The catalyst has to meet numerous requirements, depending on the specific application, such as high thermal resistance, shock resistance, sufficient surface area, negligible influence on the exhaust pressure, adequate reaction time, etc.

In case of vehicular emission, the use of platinum group metals – PGMs - is the most popular solution in emission control. The three-way catalyst is responsible for the oxidation of hydrocarbons and carbon monoxide and the reduction of nitrogen oxides [8]. The oxidation also includes some of the MCs as mentioned before PAHs, but this is not the deliberate function.

Although in theory PGMs can be used to control and decrease the concentration of organic MCs in exhausts, there are issues that prevent them from being implemented in greater quantities than at present. In the European Union, about 9 million gasoline-powered vehicles are registered each year [9], each one of them equipped with a three-way catalyst containing approximately 2 grams of PGM [10], therefore, even the smallest addition of this material will greatly increase demand and already high price. To compare, based on the prices on October 2021, platinum costs around 32$ per gram, palladium 68$, rhodium 350$, and gold costs 57 $ per gram. In addition to financial reasons, the great environmental and health benefits associated with MCs removal encourage scientists to look for alternative materials.

Several studies can be found that can be used as MCs control and removal material. Weber et al. [11] studied the decomposition of polychlorinated dibenzodioxins or PAHs on WO_3-V_2O_5 supported on TiO_2. Research of his group shows that the destruction of the selected MCs started at 100ºC. An increase in the temperature caused deposition of the by-products on the catalyst. This means that the catalyst could be used as storage for MCs, and the removal process can occur during short-term temperature increase events, above 250ºC – 300ºC.

Arunachalam et. al. [12] conducted studies on the modelling of temperatures and soot oxidation of a cerium-coated gasoline particulate filter. The filter was loaded with a predetermined amount of soot (2 g/l and 0,67 g/l). During the regeneration event, up to 50% of the organic material, including MCs, was oxidized. However, the work was not aimed at the removal of MCs.

Park et al. [13] studied the influence of Pt, Pd, and Mo on the reduction of naphthalene in diesel engine exhaust fumes. PGMs were used on the two different support materials SBA-15 and γ-alumina. The experiments were performed in the laboratory-scale on a fixed bed catalytic bed at temperatures ranged from 150ºC to 500ºC. The research focused on a single PAH, naphthalene. The studied materials show a conversion ratio of more than 95% of naphthalene to CO_2. The support used in this study has promising thermal stability and overall performance under vehicle exhaust, which indicates that this material should be further studied as a support for the MCs removal material based on the other transition metals.

In the case of combustion in stationary sources, Tseng et al. [14] studied the removal of selected MCs in flue gases from sawdust combustion. During laboratory-scale experiments, catalysts such as Co, Ni, Fe, and Cu, all supported on the activated carbon, were used for reduction of selected PAHs. The total destruction removal efficiency of the MCs differs between transition metals. The performance of Co was the best, removing 94% of the studied PAHs, iron and copper have 62% and 55%, respectively, while Ni removed 23% of MCs.

Ni Zheng et al. [15] focused on soil purification with the use of iron oxides: goethite, hematite, and maghemite. The study investigated the removal of anthracene, benzo[a]pyrene, naphthalene, and penanthrene. The degradation of anthracene in the presence of different iron oxides varies from approximately 30% in goethite, 40% in maghemite, and more than 80% in hematite during the 7-day period. The removal ability of hematie MCs was further studied over a 17-day period. The results in Table 4 show a reduction in a presence of hematite, which ranged from 55% of phenanthrene to more than 97% of naphthalene.

Table 4. Reduction of MCs in hematite [15]

α-Fe_2O_3 PAHs reduction over 17 days [%]			
Anthracene	90.1	Benzo[a]pyrene	26.7
Naphthalene	97.5	Phenanthrene	55.4

It is worth mentioning that iron is successfully used in the removal of PAHs from soil or water [16], [17] but it may be susceptible to oxidation, greatly lowering its catalytic potential.

In the case of nickel, the Raneys form can be used for a highly selective reduction of PAHs in a hydrogenation reaction [18]. Organic MCs, such as anthracene, might be reduced to octahydroanthracenes. Although the anthracene derivative is still harmful to the environment, it is safer than its initial form. Although complete oxidation to CO_2 and H_2O is desirable, partial reduction of toxicity might be satisfactory. The Raneys nickel is also prone to oxidization under the influence of atmospheric air; therefore, nickel should be used with a proper catalytic bed, rather than in Raneys form. In addition to cordierite, SBA-15, γ-alumina [13] or fujasite [19] can be used.

Partial oxidation of PAHs can lead to an increase in the concentration of CO in the exhaust gas [19]. This might give false evidence of the performance of the modified material, while the overall fume toxicity will be decreased.

5 Conclusions

The majority of the studies conducted so far focused on the regulated emission due to favorable cost-effectiveness ratio. Numerous acts and laws such as European Emission Standards regulate the main pollutants such as CO, CO_2, NO_x etc. In case of the other, non-regulated pollutants, it is worth pointing out that:

- MCs have greater negative influence on health and environment than regulated emission, however, they are underrepresented in current air-pollution quality regulations.
- TEF can be used as a valid description of the toxicity of the exhaust components and to describe adverse influence of the MCs. The TEF should be used together with PM and PN to accurately describe negative effect of the overall pollution
- Identification of the physical and chemical properties of the MCs is important to understand and estimate total influence of the MCs on health and environment. Due to varied chemical composition the identification of the source is necessary as well.
- The studies on particles composed of PAHs, their derivatives, metals and metalloids (including heavy metals), and inorganic ions should be deepened.
- The negative impact of the individual MCs is well known, but the total influence on health, the share of selected compounds in PM, and factors that increase emission must be studied in a deeper way.
- The developed solution to reduce the MCs concentration in the exhaust gasses should not only represent the best available solution, but also be environmentally friendly, inexpensive and people-friendly.

While PGMs can be a great solution for the MCs control, their significant price renders them impractical. The materials should be inexpensive, easy to apply during production or implement into the work cycle. Depending on the application materials have to meet requirements such as thermal stability, shock resistance etc. The selectivity towards the most toxic MCs is the most desired feature of the material, due to the fact that some of the exhaust components are hundreds or even thousands of times more toxic than others.

6 References

[1] Dz.U. 2021 poz. 845 ORDINANCE MINISTER OF THE ENVIRONMENT of August 24, 2012 on the levels of certain substances in the air Appendix 1.

[2] T. Zhao, L. Yang, Q. Huang, W. Zhang, S. Duan, H. Gao, and W. Wang, PM2.5-bound polycyclic aromatic hydrocarbons (PAHs) and nitrated-PAHs (NPAHs) emitted by gasoline vehicles: Characterization and health risk assessment, *Sci. Total Environ.*, vol. 727, p. 138631, 2020, DOI: 10.1016/j.scitotenv.2020.138631.

[3] W. Pacura, K. Szramowiat-Sala, J. Gołaś, and P. Bielaczyc, Advanced analysis of solid particles, *Powertrains, fuels Lubr. Digit. summit, Pittsbg.*, 2020.

[4] K. Szramowiat, J. Woodburn, W. Pacura, K. Berent, P. Bielaczyć, and J. Gołaś, Engine-generated solid particles – a case study., *Combust. Engines*, vol. 174, no. 3, pp. 33–39, 2018.

[5] E. Zervas, X. Montagne, and J. Lahaye, C1 - C5 organic acid emissions from an SI engine: Influence of fuel and air/fuel equivalence ratio, *Environ. Sci. Technol.*, vol. 35, no. 13, pp. 2746–2751, 2001, DOI: 10.1021/es000237v.

[6] N. R. H. Bock, M. M. Baum, J. A. Moss, A. E. Castonguay, S. Jocic, and W. F. Northrop, Dicarboxylic acid emissions from a GDI engine equipped with a catalytic gasoline particulate filter, *Fuel*, vol. 275, no. October 2019, p. 117940, 2020, DOI: 10.1016/j.fuel.2020.117940.

[7] F. Rodriguez and J. Dornoff, Beyond NOx: Emission of unregulated pollutants from a modern gasoline car., *International Council of Clean Transport*. Berlin, 2019.

[8] W. Pacura, K. Szramowiat, and J. Gołaś, The gasoline particulate filters and light-duty gasoline vehicles emission, *Analityka*, 2019.

[9] ACEA, The Automobile Industry Pocket Guide, 2021.

[10] I. Yakoumis, A. M. Moschovi, I. Giannopoulou, and D. Panias, Real life experimental determination of platinum group metals content in automotive catalytic converters, *IOP Conf. Ser. Mater. Sci. Eng.*, vol. 329, no. 1, 2018, DOI: 10.1088/1757- 99X/329/1/012009.

[11] R. Weber,T. Sakurai, and H. Hagenmaier, Low temperature decomposition of PCDD/PCDF, chlorobenzenes and PAHs by TiO2-based V2O5-WO3 catalysts, Appl. Catal. B Environ., vol. 20, no. 4, pp. 249–256, 1999, DOI: 10.1016/S0926-3373(98)00115-5.

[12] H. Arunachalam, G. Pozzato, M. A. Hoffman, and S. Onori, Modeling the thermal and soot oxidation dynamics inside a ceria-coated gasoline particulate filter, *Control Eng. Pract.*, vol. 94, February 2019, p. 104199, 2020, DOI: 0.1016/j.conengprac.2019.104199.

[13] J. Il Park, J. K. Lee, J. Miyawaki, S. H. Yoon, and I. Mochida, Catalytic oxidation of polycyclic aromatic hydrocarbons (PAHs) over SBA-15 supported metal catalysts, *J. Ind. Eng. Chem.*, vol. 17, no. 2, pp. 271–276, 2011, DOI: 10.1016/j.jiec.2011.02.020.

[14] H. H. Tseng, C. Y. Lu, F. Y. Chang, M. Y. Wey, and H. T. Cheng, Catalytic removal of NO and PAHs over AC-supported catalysts from incineration flue gas: Bench-scale and pilot-plant tests, *Chem. Eng. J.*, vol. 169, no. 1–3, pp. 135–143, 2011, DOI: 10.1016/j.cej.2011.02.069.

[15] Z. Ni, C. Zhang, Z. Wang, S. Zhao, X. Fan, and H. Jia, Performance and potential mechanism of transformation of polycyclic aromatic hydrocarbons (PAHs) on various iron oxides, *J. Hazard. Mater.*, vol. 403, no. September 2020, p. 123993, 2021, DOI: 10.1016/j.jhazmat.2020.123993.

[16] D. Baragaño, J. Alonso, J. R. Gallego, M. C. Lobo, and M. Gil-Díaz, Magnetite nanoparticles for the remediation of soils co-contaminated with As and PAHs, *Chem. Eng. J.*, vol. 399, May, p. 125809, 2020, DOI: 10.1016/j.cej.2020.125809.

[17] M. Hosseinpour, M. Akizuki, Y. Oshima, and M. Soltani, Influence of formic acid and iron oxide nanoparticles on active hydrogenation of PAHs by hot compressed water. Isotope tracing study, *Fuel*, vol. 254, no. April, p. 115675, 2019, DOI: 10.1016/j.fuel.2019.115675.

[18] A. A. Philippov, A. M. Chibiryaev, and O. N. Martyanov, Catalyzed transfer hydrogenation by 2-propanol for highly selective PAHs reduction, *Catal. Today*, vol. 379, pp. 15–22, 2021, DOI: 10.1016/j.cattod.2020.06.060.

[19] S. C. Marie-Rose, T. Belin, J. Mijoin, E. Fiani, M. Taralunga, F. Nicol, X. Chaucherie, and P. Magnoux, "Catalytic combustion of polycyclic aromatic hydrocarbons (PAHs) over zeolite type catalysts: Effect of water and PAHs concentration," *Appl. Catal. B Environ.*, vol. 90, no. 3–4, pp. 489–496, 2009, DOI: 10.1016/j.apcatb.2009.03.035.

TREATMENT OF MUNICIPAL WASTEWATER BY ELECTROCOAGULATION AND NATURAL ZEOLITE – INFLUENCE OF INITIAL pH VALUES

Nediljka Vukojević Medvidović[1,*]; Ladislav Vrsalović[1]; Tali Brozinčević[1]; Sandra Svilović[1]

[1] Faculty of Chemistry and Technology in Split, Croatia
[*] corresponding author e-mail: nvukojev@ktf-split.hr

Abstract. *Treatment of municipal wastewater prior to discharge into the environment is necessary to prevent pollution. In order to obtain satisfactory effluent quality, integration of two or more physical, chemical or biological process operations after primary treatment is needed. In this paper, the municipal wastewater is treated with electrocoagulation integrated with sorption on natural zeolite. Experiments are performed in an electrochemical cell with aluminium electrodes under conditions of I = 0.1 A, U = 29.9 V, with the addition of zeolite at the solid/liquid ratio of 20 g/l, and contact time of 60 min. The influence of initial pH values on removal efficiency has been investigated. The pH value, el. conductivity, temperature, turbidity, chemical oxygen demand (COD) and total Kjeldahl nitrogen (TKN) were used to evaluate removal efficiency. Results show that reductions in el. conductivity and COD are independent of adjustment of the initial pH values of wastewater. However, the initial pH of wastewater does have a significant influence on reducing the turbidity and TKN. The increase in solution temperature is higher in an acidic medium, which relates to higher electrode consumption and operational cost. Results confirm that the initial pH of wastewater has a significant impact on municipal wastewater treatment by electrocoagulation integrated with zeolites.*

Keywords: *municipal wastewater integrated process treatment, electrocoagulation, natural zeolite*

1 Introduction

Municipal wastewaters are usually defined as a mixture of wastewater from household and industrial activity. Their compositions depend on living standards, climate, water supply systems, availability of freshwater, and industrial wastewater composition. Typical municipal wastewater is characterized by organic load, suspended solids, nutrients and pathogens, and they are mostly biodegradable. The pollutants from industry can be categorized as potentially toxic elements (such as heavy metals) and organic pollutants, which vary from easily biodegradable to highly persistent. In coastal areas, intrusions of salty seawater into sewage occur, which also influence on the composition of municipal wastewater [1, 2]. Due to complex composition, municipal

wastewater is often very difficult to treat with classical biological processes after primary processing, thus additional physical or/and chemical process is needed. Recently, researches have been focused on the integration of two or more physical, chemical or biological processes treatment to obtain an effluent of satisfactory quality.

Electrocoagulation is defined as the process that forms coagulant trough electrodissolution of a sacrificial anode, usually aluminium or iron, which destabilized various pollutants. Destabilized pollutants aggregate into flocs. Formed flocs can be removed from the solution due to electroflotation with hydrogen gas produced at the cathodes or are under process of flotation or sedimentation [3].

Natural zeolites are already recognized as ion exchangers, adsorbents and sieve molecules. Their natural and modified forms can efficiently remove heavy metals, ammonia, radioactive ions, inorganic anions and microorganisms. Due to the availability of their deposit in nature, simplicity of exploitation and environmental compatibility, they are widely used in wastewater treatment and environmental remediation purposes [4]. In this paper, the treatment efficiency of municipal wastewater with electrocoagulation and simultaneous sorption on natural zeolite at different initial pH values is performed to achieve satisfactory effluent quality.

2 Experimental studies

Municipal wastewater was sampled at the outlet of oil/grease aerator from the wastewater treatment plant in Split, Croatia. Characterization of initial sample was performed by pH value, el. conductivity, turbidity, temperature, chemical oxygen demand (COD), biochemical oxygen demand (BOD) and Kjeldahl nitrogen (T_{KN}) determination.

Natural zeolite (NZ), clinoptilolite, used in this study was originated from Zlatokop deposit, Vranjska Banja, Serbia, of granulation of 0.1-0.5 mm. The characterization of zeolite was previously published [4].

Electrocoagulation was performed in an electrochemical cell under the current intensity and applied voltage of I = 0.1 A, U = 29.9 V, respectively. The cell was filled with 250 ml of wastewater solution and immersed aluminium AA2007 alloy electrodes (height: width: thickness = 5.9: 1.9: 0.6 cm), with the distance between the electrodes of 3 cm. Influence of initial pH values of solution (without initial pH adjustment and with pH adjustment at pH=9 and pH=4) on electrocoagulation efficiency was investigated, at a contact time of t = 60 min. During the experiment, the solution was mixed with gentle stirring with a magnetic stirrer, without the addition of electrolyte. In the EC experiments with the addition of zeolite (marked as EC_Z), the mass of added zeolite was 5 g per 250 mL of effluent (solid to liquid ratio 20 g/L). Between each experiment, the electrodes were ground and polished with successive wet SiC emery papers (up to 800 grit), ultrasonically clean in 70% ethanol and deionised water. The pH value, temperature and electrical conductivity were monitored, and after the experiment, the pH value, electrical conductivity, temperature, turbidity, chemical oxygen demand (COD) and total Kjeldahl nitrogen (TN_K) were determined.

3 Results and discussion

Table 1 gives physical-chemical analysis of municipal wastewater compared with maximal allowed values according to the Croatian Regulation [5].

Results show that municipal wastewater is characterized with medium organic load, ammonia concentration, conductivity and turbidity, while the pH value is within the limit values prescribed

by the Croatian Regulation [5]. Although el. conductivity limits are not defined by Croatian Regulation, it is well known that discharge of wastewater with high EC into the surrounding watershed may bring water imbalance for aquatic organisms and could greatly decrease dissolved oxygen concentration [2]. The low value of the BOD_5/COD ratio indicates the presence of slowly biodegradable organic components in municipal wastewater. Thus, further treatment with physio-chemical process is suggested.

Table 1 Municipal wastewater characterization.

Parameter	Municipal wastewater	Natural surface waters [5]	Public sewage system [5]
pH	8.18	6.5-9.5	6.5 – 9.5
Temperature, ºC	18	30	40
El. cond., µS/cm	953	-	-
Turbidity, NTU	11.7	-	-
COD, mgO_2/l	353.89	125	700
BOD_5, mgO_2/l	61.06	25	250
BOD_5/COD	0.173	-	-
TN_K, mg N/l	58.83	15*	50*
Note* - values for total nitrogen are compared since values for Kjeldahl nitrogen are not specified by Croatian Regulation [5]			

3.1 Comparison of pH, el. conductivity and temperature during electrocoagulation

Municipal wastewater was treated by electrocoagulation, at condition without pH adjustment of solution and with pH adjustment at pH=4 and pH=9. Results of monitoring of pH, el. conductivity and temperature during the electrocoagulation process, without and with the addition of zeolite are compared in Fig. 1-3.

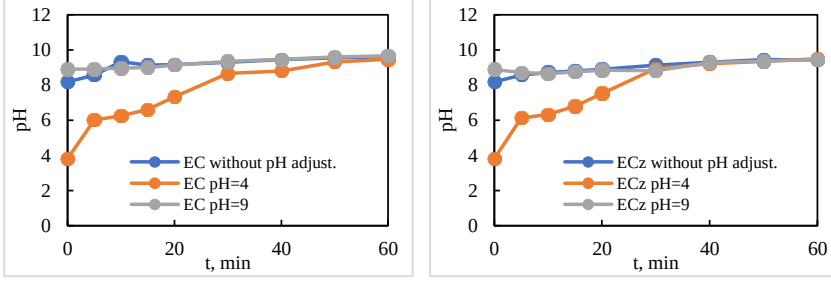

a) b)

Fig. 1 Continuous measurement of pH values in suspension at different initial pH values of wastewater during: a) electrocoagulation (EC), b) electrocoagulation with the addition of zeolite (ECz).

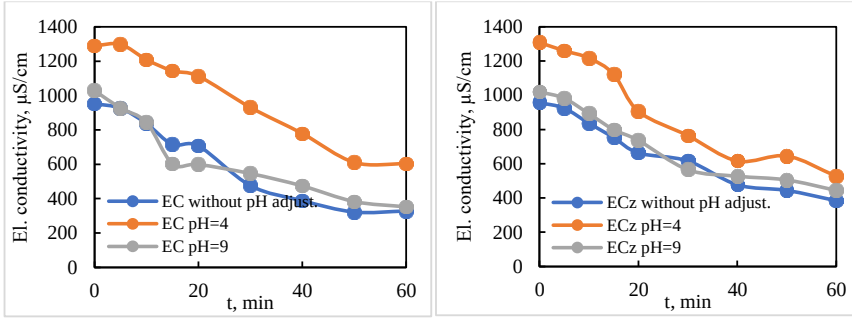

Fig. 2 Continuous measurement of el. conductivity in suspension at different initial pH values of wastewater during: a) electrocoagulation (EC), b) electrocoagulation with the addition of zeolite (EC_Z).

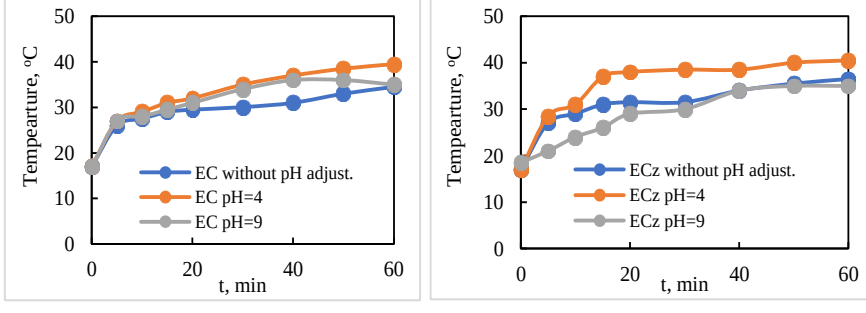

Fig. 3 Continuous measurement of temperature in suspension at different initial pH values of wastewater during: a) electrocoagulation (EC), b) electrocoagulation with the addition of zeolite (EC_Z).

In an experiment without pH solution adjustment (pH=8.18) and with adjustment at pH=9 (alkaline environment), both pH curves continuously increase (Fig 1a) and they are almost overlapping, due to very similar initial pH values. In an acidic environment (initial pH solution adjustment at pH=4), the increase of pH is more pronounced. The rise in pH is due to the process of hydrolysis of water at the cathode, which produces OH^- ions and hydrogen gas [6]. Decrease in el. conductivity is observed in all experiments, and is attributing to pollutant removal into floc by electrocoagulation.

Zeolites are well known to have the ability to neutralize the solution pH and reduce conductivity in the solution due to capturing contaminates. Results in this paper indicate that the addition of zeolite (Fig 1b and 2b) caused only a small change in final pH and final values of el. conductivity. Also, the addition of zeolite particles didn't act abrasively on the electrodes and did not contribute to cleaning the electrode surface from organic layer, as we expected. The reason for this is probably the specific composition of municipal wastewater. Namely, high values of el. conductivity shows that inorganic ions are in abundance in municipal wastewater [2], while a presence of biodegradable organic compound is not so high (see Table 1). Thus, the formation of organic layer on Al electrode by complexing aluminium with organic compounds was not observed. Contrary to these results, during treatment of biowaste leachate by electrocoagulation

integrated with zeolite, addition of zeolite particles did act abrasively on the electrodes and contribute significantly to cleaning the electrode surface from adsorbed organic layer [7].

During electrocoagulation, a continuous increase in solution temperature is recorded (see Fig. 3.a and 3.b). The increase of temperature is higher in an acidic medium (pH=4) up to 39.5-40.5ºC, which relates to higher electrode consumption at these pH values (see Table 2.). In alkaline medium, this increase is less pronounced, up to 34.5-36.5ºC. The addition of zeolite did not cause a significant change in temperature increase. Before discharging treated wastewater into the natural recipient, increasing solution temperature should be considered to avoid thermal pollution. An increase in solution temperature can be controlled by reducing the ratio of the electrode surface / solution volume.

3.2 Analysis of the efficiency of electrocoagulation

Results of turbidity, COD and Kjeldahl nitrogen before and after wastewater treatment by electrocoagulation process without and with the addition of zeolite (addition of zeolite marked as EC_Z), are compared in Fig. 4-6. In Table 2, a comparison of the removal efficiency α (%) by coagulation and electrocoagulation without and with the addition of zeolite is given. Calculated removal efficiencies for el. conductivity, turbidity, COD and T_{KN} are summarized in Table 2.

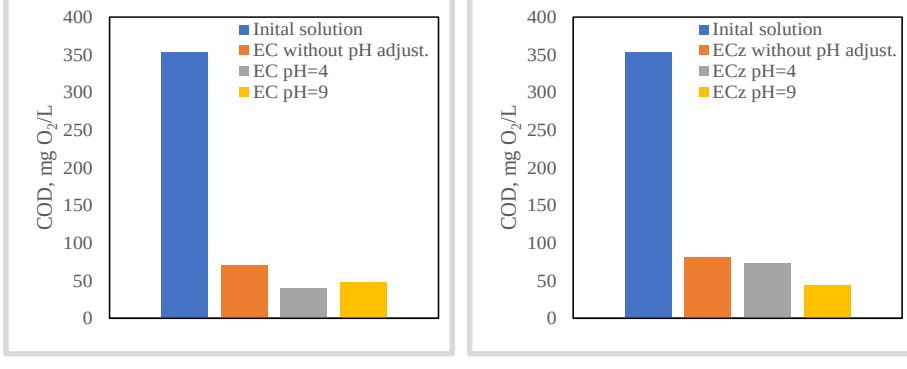

Fig. 4 COD values in initial solution and suspension, at different initial pH values, after: a) electrocoagulation, b) electrocoagulation with the addition of zeolite.

Table 2 Removal efficiency for reduction of el. conductivity, turbidity, COD and TK_N.

Experiment	Removal efficiency, %			
	El. cond.	NTU	COD	TK_N
EC $_{\text{without pH adjust.}}$	65.58	88.21	80.21	52.38
$EC_{Z\ \text{without pH adjust.}}$	59.87	80.51	77.08	76.19
EC $_{\text{pH=4}}$	53.26	97.44	88.54	76.19
$EC_{Z\ \text{pH=4}}$	59.71	62.14	79.17	52.38
EC $_{\text{pH=9}}$	65.79	84.96	86.46	42.86
$EC_{Z\ \text{pH=9}}$	56.47	82.05	87.50	61.90

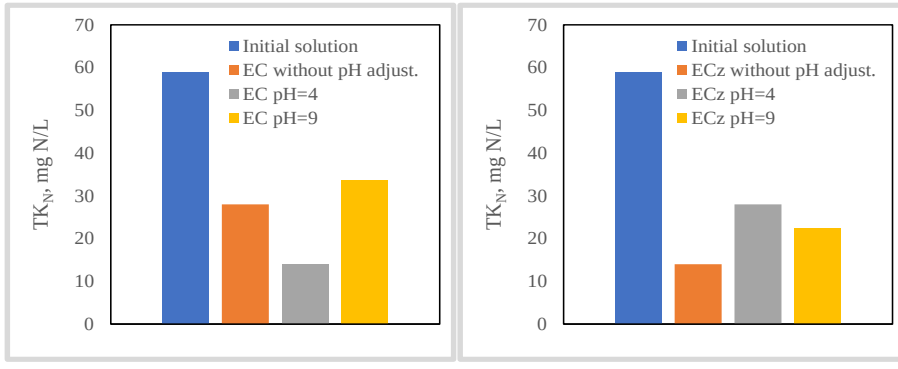

Fig. 5 Kjeldahl nitrogen values in initial solution and suspension, at different initial pH values, after: a) electrocoagulation, b) electrocoagulation with the addition of zeolite.

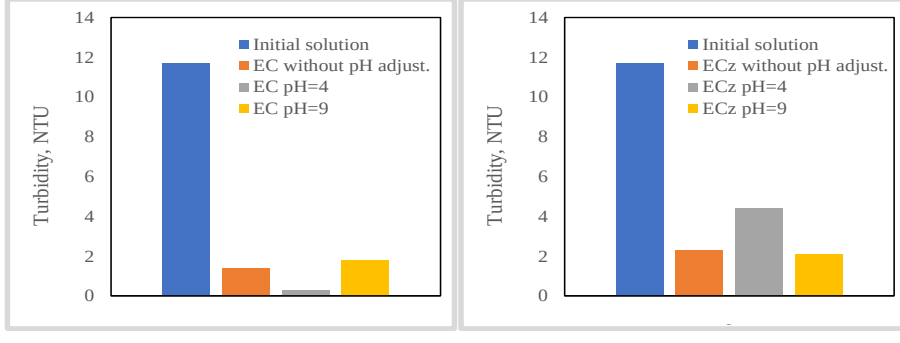

Fig. 6 Turbidity values in initial solution and suspension, at different initial pH values, after: a) electrocoagulation, b) electrocoagulation with the addition of zeolite.

Results show that adjustment of initial pH values doesn't have a significant effect on reduction in el. conductivity, and removal efficiency varies in range 53.26-65.79 %.

Turbidity achieves almost similar results in solution without adjustment and with adjustment of initial pH at pH=9 (80.51-88.21%). At pH=4, the highest reduction of turbidity is achieved (97.14%) while the addition of zeolite negatively affects turbidity removal efficiency (62.14%).

Reduction in COD is almost similar in all experiments and the addition of zeolite did not cause significant improvement. Results of removal efficiency expressed in COD are varying in the range 77.08-88.54 %.

Reduction of Kjeldalh nitrogen is depending on the initial pH and the addition of zeolite. In an acidic environment, better TK_N removal is obtained without the addition of zeolite (76.19%), while in alkaline environment, the addition of zeolite shows higher TK_N removal percentage (in the experiment without pH adjustment, the increase is from 52.38-76.19%; while in the experiment with pH adjustment at pH=9, the increase is from 42.86-61.90%). Namely, in an alkaline solution, the $Al(OH)_4^-$ coagulant occur, which is characterised by lower coagulation efficiency [3]. Thus, the addition of zeolite has a positive effect on TK_N removal. In an acidic

environment, aluminium species with better coagulation ability occur, causing better turbidity removal, thus the addition of zeolite is not suggested.

3.3 Comparison of the mass of Al electrodes consumed during the experiment

Before and after immersion, the electrodes are weighed on an analytical balance, and results are given in Table 3. The highest consumption of the anode is in an acid environment (at pH=4), which will influence on operation cost. In an alkaline environment, the addition of zeolite is suggested as it influences on smaller consumption of electrode. The results also confirm that Al was dissolved not only from the anode but also from the cathode, which is in agreement with reference [8].

Table 3 Mass of Al electrodes consumed during the experiment.

Experiments	Mass of Al electrodes consume during the experiment, g	
	Anode	Cathode
EC without pH adjust.	0.1018	0.0234
EC_Z without pH adjust.	0.0852	0.0157
$EC_{pH=4}$	0.1570	0.0051
$EC_{Z\ pH=4}$	0.1590	0.0191
$EC_{pH=9}$	0.0803	0.0119
$EC_{Z\ pH=9}$	0.0758	0.0143

4 Conclusion

The treatment of municipal wastewater by electrocoagulation integrated with sorption on natural zeolite is dependent on initial pH values. The increase of pH is more pronounced in an acidic environment, due to OH^- production at the cathodes. The rise in temperature is higher in an acidic medium, which is connected with higher electrode consumption and operational cost. Decrease in el. conductivity is independent of initial pH values of the solution, which is attributed to pollutants removal by electrocoagulation into floc. Adjustment of initial pH values doesn't have a significant effect on reduction in el. conductivity and COD. However, in an acidic environment, the highest reduction of turbidity (97.14%) and TK_N (76.19%) is obtained without the addition of zeolite, as aluminium species with better coagulation ability occur. In alkaline solution, the $Al(OH)_4^-$ coagulant occurs, characterised by lower coagulation efficiency. Thus the addition of zeolite has a positive effect on TK_N removal from municipal wastewater in an alkaline environment.

Results confirm that initial pH has a significant influence on municipal wastewater treatment by electrocoagulation integrated with zeolites. Even satisfactory values of effluent quality are obtained, increased values of solution temperature above the limits prescribed by Croatian regulation need to be solved before discharging treated wastewater into a natural recipient, in order to avoid thermal pollution.

References

[1] Pollutants in urban wastewater and sewage sludge, European Communities, 2001, https://ec.europa.eu/environment/archives/waste/sludge/pdf/sludge_pollutants.pdf [accessed 20.08.21]

[2] Aniyikaiye T. E., Oluseyi T., Odiyo J. O., Edokpayi J. N., Physico-Chemical Analysis of Wastewater Discharge from Selected Paint Industries in Lagos, Nigeria, Int. J. Environ. Res. Public Health 2019, 16, 1235; DOI: 10.3390/ijerph16071235

[3] Tawalbeh M, Al-Shannag M., Al-Anber Z., Bani-Melheme K., Combined electrocoagulation processes as a novel approach for enhanced pollutants removal: A state-of-the-art review, Sci. Total Environ 744 (2020), 140806.

[4] Vukojević Medvidović N., Lead removal on natural zeolite clinoptilolite – column process modelling, Doctoral thesis, Faculty of Chemistry and Technology in Split, Split, 2007.

[5] Regulation on emission limits values in wastewater, NN 26/2020 (in Croatian).

[6] Oreščanin V., Kollar R., Nađ K., Electrochemical tretament of wastewater from potato chips production, Hrvatske vode, 24 (2016) 95, 129-142 (in Croatian).

[7] Vukojević Medvidović N., Vrsalović L., Ugrina T., Jukić I., Electrocoagulation augmented with natural zeolite – the new hybrid process for treatment of leachate from composting of biowaste, In: Dolić N., Zovko Brodarac Z., Brajčinović S. (eds). Proceedings of the 19th International Foundrymen conference: Humans – Valuable Resource for Foundry Industry Development, University of Zagreb, Faculty of Metallurgy, 2021, p. 489-498.National Waste Management Plan 2022. Republic of Poland. Resolution No 88 of the Council of Ministers of 1 July 2016 (item 784)

[8] Ghernaouta, D., Ghernaoutb, B., Boucherita, A., Naceura, M.W., Khelifaa, A., Kelli, A., Study on mechanism of electrocoagulation with iron electrodes in idealised conditions and electrocoagulation of humic acids solution in batch using aluminium electrodes, Desalin. Water Treat., 8 (2009) 91-99. DOI: 10.5004/dwt.2009.668.

INFLUENCE OF RAILWAY VIBRATION ON BUILDING AND PEOPLE

Filip Pachla[1,*]; Alicja Kowalska-Koczwara[1]; Tadeusz Tatara[1]

[1] Cracow University of Technology, Department of Structural Mechanics and Materal Mechanics, Warszawska 24, 31-155 Kraków, Poland
* corresponding author: fpachla@pk.edu.pl

Abstract. *According to the construction law. railway vibrations are classified as environmental pollutants and should be taken into account when designing buildings. The Design of buildings in modern times seems to be a fully recognized topic. There are many national and international standards and guidelines. which should be taken into account. For these reasons designers could have some problems. especially when there is a problem with vibrations in the surrounding area. They do not know which standard should be used and there are problems in guidelines themselves- there is many imprecise definitions in standards regulations. This may result of not many mistakes made during dynamical analysis of the structure. For example in ISO standard there is a definition of duration of vibration: "the recorded signal should be sufficient to ensure rational statistical accuracy". which means nothing. According to Polish code (PN-B-02171:2017-06) duration of vibration is the range in which the value of vibration acceleration amplitudes does not fall below 0.2 of the maximum amplitude value in the recorded waveform – this definition is more precise. It is worth noting that in the seismic areas and in the relation to the slender structures the dynamical design is much better recognize than for transport vibrations. especially in relation to buildings. Differences in the regulations and ignorance in the aspect of dynamical design of the buildings. They often lead to errors in the design of buildings subjected to transport influences for example coming from railways. In this paper an example of such situation is analysed and the recommendations are given.*

1 Introduction

The aim of this paper is to analyzed how railway vibrations influence on the building design. There are two aspects of vibrational influence on building design. the first is influence on building structure [3-4] and the second which mainly influence on design of the building is human perception of vibration [5-7]. Human perception of vibration could be the basic parameter in designing new buildings subjected to different type of transport vibrations. Humans are more sensitive for vibrations then building structure.

The building chosen for analysis is a single-family building located near the railway line about 32 m far. It was designed with a longitudinal axis perpendicular to the axis of the track The building's structure is traditional. It was designed as a brick with monolithic reinforced concrete ceilings. with unidirectional or cross reinforcement system. The foundations were designed in the form of reinforced concrete benches. Similarly. foundation walls are also reinforced concrete. Masonry walls made of Porotherm ceramic airbricks. All lintels with larger spans were made as monolithic reinforced concrete. According to the current line characteristics. the speed limit for trains depends on their types and is:

- Passenger trains: Vmax = 160 km/h
- Cargo trains: Vmax = 120 km/h

Representative extortions from a railway line with similar characteristics and purpose were selected for analysis.

2 Methods

The FEM model was build according to design documentation. Structural elements such as beams and columns were modeled with beam-type finite elements (a two-node finite element with 6 degrees of freedom in a node). while surface elements such as walls and ceilings with shell elements (a four-node or three-node finite element with 6 degrees of freedom in a node). The model is shown in Fig. 1.

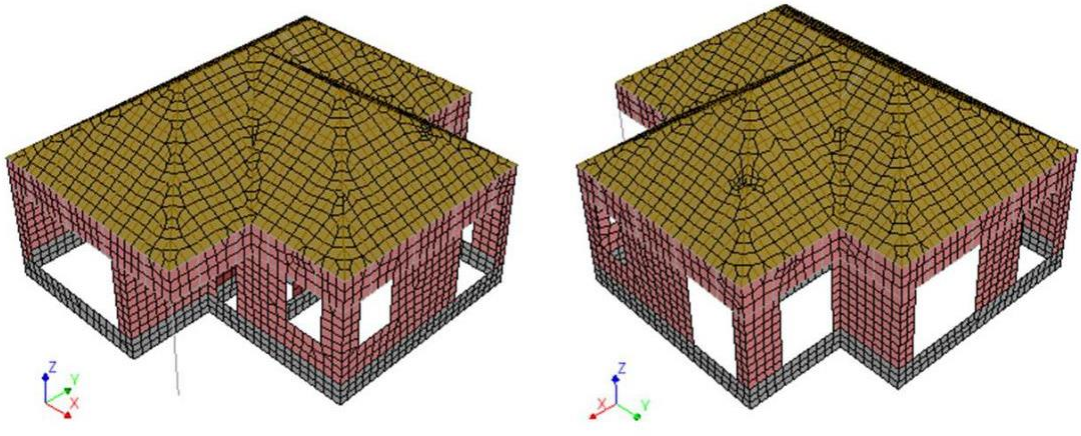

Fig. 1. FEM model of the analysed building

For the entire structure. global damping was adopted as critical equal 5%. which corresponds to traditional masonry buildings. The calculations were made using the direct integration method of equations of motion assuming an integration step $\Delta t = 0.0009765625$s. which corresponds to a sampling signal of 1024 Hz. Kinematic excitations were adopted in the form of recorded accelerations applied at the foundation of the model (building contact with the ground) as uniform excitation. The four scenarios of excitation were analyzed: cargo train. pendolino train with the speed of 160km/h. pendolino with the speed of 200 km/h and old high speed train passing. The examples of signals are shown in Fig. 2.

The following materials characteristics were adopted:

- Concrete (Reinforced concrete) C16 / 20 (B-20): Young's modulus E = 29.0 GPa. Poisson's ratio $\nu = 0.2$. mass density $\rho = 2500$ kg / m^3.
- Concrete (Reinforced concrete) C25 / 30 (B-30): Young's modulus E = 31.0 GPa. Poisson's ratio $\nu = 0.2$. mass density $\rho = 2500$ kg / m^3.

- Porotherm block (fb = 15MPa. fm = 5MPa): Young's modulus E = 3.9 GPa. Poisson's ratio ν = 0.25. mass density ρ = 1350 kg / m^3.Wood C-24: Young's modulus E = 11.0 GPa. Poisson's ratio ν = 0.3. mass density ρ = 420 kg / m^3.

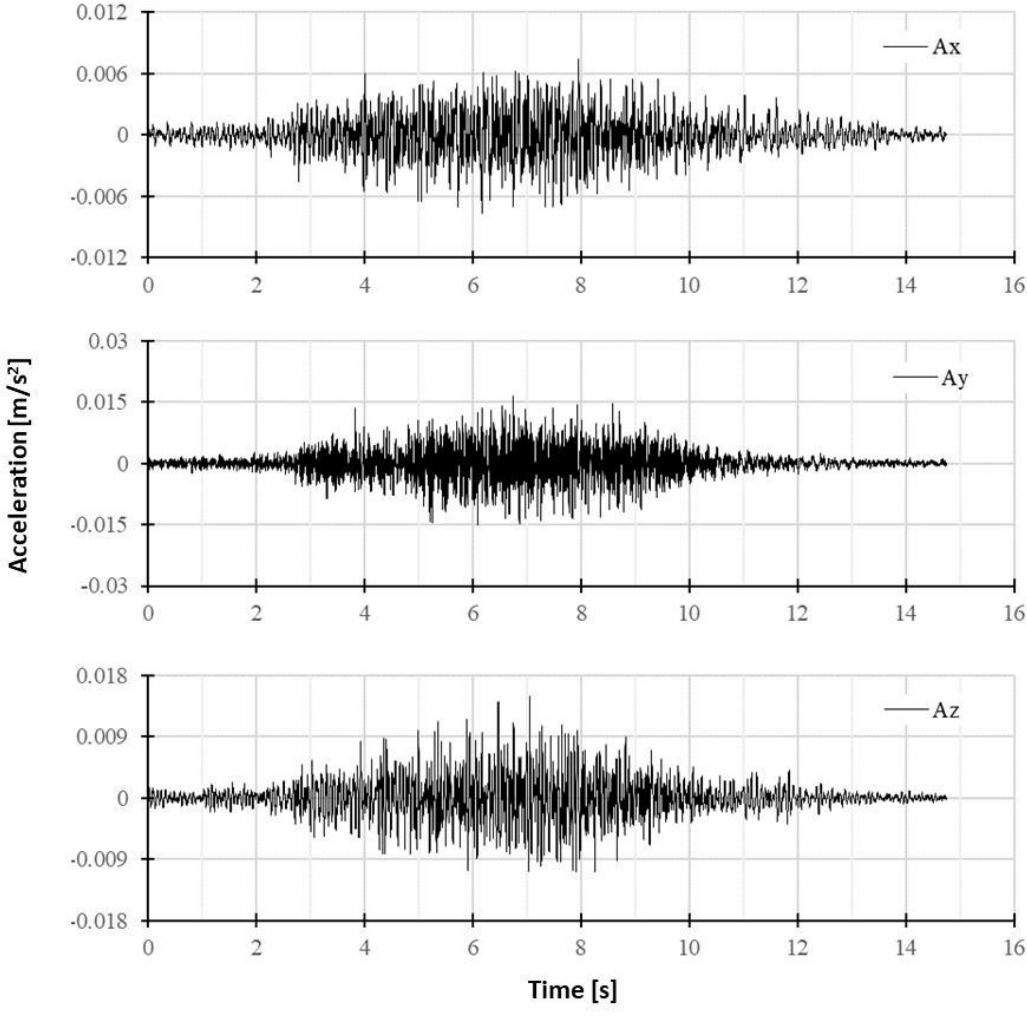

Fig. 2. Excitation in three directions

3 Results and discussion

Dynamic calculations were made on building model and on this basis the maximum equivalent stresses according to HMH (i.e. according to the Huber-Mises-Hencky effort hypothesis) were obtained in all structural elements and they were compared with the characteristic strengths of these elements. The criterion for evaluation of the vibration influence

on the building structure was assumed that if the maximum contribution of equivalent stress caused by kinematic excitation is less than 5% of the material strength. then such impact is considered as imperceptible by the building. Results of the vibration influence on building structure is listed in Table 1. Railway vibrations influence on structural elements.

Table 1. Results of the vibration influence on building structure

Type of train passing	Stress σHMH [MPa]		
	Reinforced concrete	Masonry element	Wooden element
	σdop = 1.3 MPa	σdop = 0.2 MPa	σdop = 14 MPa
Cargo 80 km/h	0.029	0.009	0.024
Pendolino 160 km/h	0.029	0.008	0.053
Pendolino 200 km/h	0.029	0.008	0.040
Old type high speed 160 km/h	0.013	0.004	0.018

For human perception of vibration RMS method was used with HPVR ratio (human perception of vibration ratio) acc. [2]. The example of such analysis is shown in Fig. 3. In the all analyzed scenarios there is a problem with z direction for human perception of vibration – the perception threshold is exceeded. Although the comfort level is not exceeded it should be remembered that in such situation vibration could be annoying for residents.

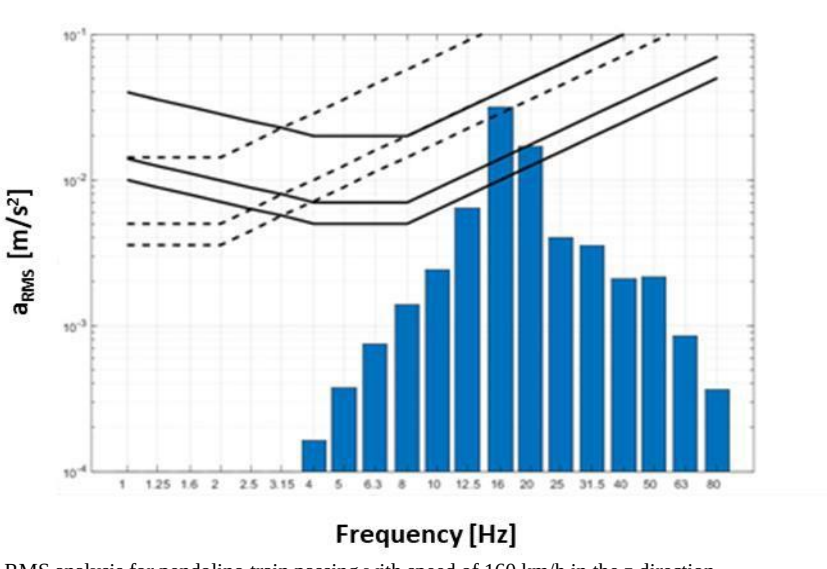

Fig.3. RMS analysis for pendolino train passing with speed of 160 km/h in the z direction

4 Conclusions

The main purpose of the work was to determine the vibrational influence on the designed single-family house with respect to human perception of vibration. Calculations on the FEM model were made in the time domain regarding the influence of vibration on the structure of the building and the human perception. The four possible scenarios were investigated. As could be seen from Table 1 all types of the trains passing near the building (about 32 m) do not influence on structural elements of the building. The thesis is confirmed that the human perception of

vibration in buildings can be a decisive design parameter for buildings located close to railways. Although the vibrational comfort level was not exceeded the vibrations which appear in this building could be annoying for residents. because perception threshold of vibration was exceeded in all four scenarios. For this reason the owner of the building decides to reduce vibrations in the building and protect himself and his family. The floor structure was modified to improve the comfort of people in the building and to ensure that the vibrations are below the threshold of human perception. The calculations and analyzes carried out in order to increase the vibrational comfort of people in the building result in the need to increase the class of structural concrete from the designed C16 / 20 (B20) to C25 / 30 (B30). increase the thickness of the floor slab to 22cm and use vibro-insulation mats at foundation level.

References

[1] International Organization for Standardization. ISO 2631-1. (1997) Mechanical vibration and shock: Evaluation of human exposure to whole-body vibration - Part 1: General requirements

[2] PN-B-02171:2017-06. Evaluation of vibrations influence on people in buildings. (2017) Polish Standard (in Polish).

[3] Hong Junqing Liu Weiqing. ANALYSIS OF EFFECTS INDUCED BY SUBWAY TRAIN ON SURROUNDING BUILDING VIBRATION《Journal of Vibration and Shock》 2006-04.

[4] Hunaidi Osama. Traffic vibrations in building. 2000. National Research Council of Canada

[5] I.H. Turunen-Risea .A. Brekkeb .L. Harvikc .C. Madshusc.R. Klæboe. Vibration in dwellings from road and rail traffic —Part I: a new Norwegian measurement standardand classification system. Applied Acoustics 64 (2003) 71–87

[6] David Waddington. James Woodcock. Michael G Smith. Sabine Janssen & Kerstin Persson Waye (2015) CargoVibes: human response to vibration due to freight rail traffic. International Journal of Rail Transportation. 3:4. 233-248

[7] David P. Connolly. Grzegorz P. Marecki. Georges Kouroussis. Ioannis Thalassinakis. Peter K. Woodward. The growth of railway ground vibration problems — A review. Science of The Total Environment. Volume 568. 15 October 2016. Pages 1276-1282

THE IMPACT OF COVID-19 ON NATURAL GAS DEMAND AND SECURITY OF SUPPLY IN POLAND

Michal Andrzej Kumor[1,2]*; Stanisław Porada[1]

[1] AGH University of Science and Technology, Faculty of Energy and Fuels, Department of Fuels Technology, Mickiewicza Av. 30, 30-059 Krakow, Poland
[2] PKN ORLEN S.A., Gas Trading Support Department, Bielanska 12, 00-085 Warsaw, Poland
* corresponding author: mickum@agh.edu.pl

Abstract. *The first case of COVID-19 infection in Poland took place in March 2020. Two significant waves of infections have passed through the country during the last 19 months. First of them at the turn of October and November 2020, and the other from February to April 2021. It is worth noting that the first wave coincided with the beginning of the 2020/2021 gas winter season. The second, was in line with its ending. The work attempts to find the answer the following question: how did the pandemic affect the consumption of natural gas (NG) by end users in Poland and did the plans for the development of the Polish transmission networks presented before the pandemic change significantly? The work also touches on the aspect of guaranteeing the security of supplies by using UGS. In order to answer the aforementioned questions, a study of the daily consumption of NG by end users connected to the transmission and distribution network was conducted. The analysis covered two groups of natural gas transported by the transmission network operator, i.e. low-methane gas - Lw and high-methane gas - E. The observed results indicate an increasing demand and undisturbed development of the NG sector in Poland, in particular for large high-methane NG end users connected to high pressure transmission network. The extremely frosty months like: March and April 2021 had the crucial impact on the largest ever consumption of distribution networks. Despite the lower consumption in 2020, compared to the assumptions from before the pandemic, at the end of 2021 the level of NG consumption from both groups will approach the published optimal development scenario. Historically based forecasts confirm the high probability of the implementation of one of the 3 development plans presented in 2019. In the UGS at the end of the withdrawal season, more fuel was stored than in the previous 4 years. Higher inventories of storage facilities allowed to accelerate the injection process during the summer season*.

Keywords: *Polish gas market, natural gas, COVID-19, UGS, development plan*

1. Introduction

The COVID changed our lives. Society spends more time at home, people can work from home. The European Comission quarterly report on the European Gas Markets with a special

focus on the impact of COVID-19 on the global LNG market presented decreasing demand for natural gas [1]. The biggest decreases during three quarters of 2020 could be observed in Italy (-8%), Germany (-5.5%). In the first three quarters of 2020 gas consumption in the EU was down by 5%. The International Energy Agency reported 4% decrease in natural gas demand in global market and 7% decrease in natural gas demand in European market [2]. Polish Economic Institute determined the level of decrease in electricity demand by 15% [3]. Can the change in people's lifestyle resulting from the COVID-19 restrictions affect the natural gas (NG) market in Poland?

2. Aim of the study

The article is divided into three parts. The first part deals with registered changes in the demand for natural gas by end users during the pandemic. The pandemic period covers almost 19 consecutive gas months (570 days) from 2020.03.01 to 2021.09.30. The second part of the article deals with the possibility of creating natural gas inventories in underground gas storages in Poland. Recorded levels of natural gas inventories in storage facilities during the pandemic are confronted with historical levels. Third part of the article will answer the question about the development plans of the natural gas sector in Poland and their assumptions from 2019. 3 dynamic forecast variants of natural gas consumption until 2023 were prepared. Study based on the historical billing data and calculated dynamics of changes in natural gas demand during 2089 days.

3. Methods

The first case of COVID in Poland took place in March 2020. Levels of natural gas demand are official publicated by Transmission System Operator Gaz-System S.A. billing data [4]. For the analysis were chosen 2089 days from 2016.01.01 to 2021.09.20 with special attention to 570 days from 2020.03.01 to 2021.09.20. 570 days are the main test sample. Data from January 2016 to February 2020 are the historical benchmark- reference points for the analysis.

Two groups of natural gas were used for the analysis. The first is a high methane gas with high methane content and trace amounts of nitrogen [5]. Group E, high metan content, high calorific natural gas is a part of the global market and can be imported by pipelines from other EU or non-EU countries, by LNG carriers and sourced also from domestic production [6]. The second group is a low methane gas with a higher nitrogen content. This gas with lower calorific value comes from domestic production only [5]. To complete the analysis, measured demand should be confronted with the recorded and historical temperatures [7,8]. Polish gas transmission system with high pressure pipelines is characterized by similar and flat demand all over the year. This system is resistant to temperature changes. The second analyzed system is distribution system. It is used to deliver fuel to household use: cooking, heating water and also for small industry, especially used by local heating plants. What is important, the characteristics of consumption by end users in this system have a flat part and a seasonal part, which is strongly related to the recorded temperature [9]. Temperature is the main factor driving the demand for natural gas in lower pressures networks. A comparative analysis of historical data and data from the period of COVID-19 pandemic was conducted. A comparative analysis of historical UGS inventories and data from the period of COVID-19 pandemic was conducted too. Data for this part of research were imported from GIE AGSI+ [10].

Last part of the research is focused on the development plans and the implementation of their assumptions [11]. In order to prepare a comparison of the demand with the development plans, it was necessary to prepare forecasts of natural gas consumption for 2022 and 2023. Three forecasts were prepared;

1. Optimistic- using maximum relative increases in natural gas demand from the period 2016-2020,
2. Normal- using average relative increases in natural gas demand from the period 2016-2020,
3. Pessimistic- using minimum relative increases or decrease in natural gas demand.

To calculate 2021 demand billing data for months from January to September were used. Forecasts were calculated only for the last quarter of 2021. It is worth noting that the forecasts were prepared separately for the distribution and transmission system end users. It is important to underline, that there are many drivers creating gas demand. Besides temperature, there are gas prices, energy prices, CO_2 emission prices and coal prices. They can be used to calculate clean dark spread (for coal) and clean spark spread (for natural gas). These factors are helpful in choosing more profitable energy source and with appropriate price correlation can affect the natural gas demand [12].

4. Results

It is worth pointing out that natural gas Lw (low methane) demand by end users from transmission and distribution system in 2020 was 6,6 [TWh]. High methane natural gas demand was 194,5 [TWh] so more than 29 times higher than Lw [13]. Both natural gas groups were characterized by similar shape of demand curves during the tested period. Low methane NG group cannot significantly affect the whole country demand and will not be described in details in this document.

4.1 Distribution System

Natural gas distribution system is characterized by seasonality – fig.1. Natural gas demand in winter can twice the size than during summer months. The grey channel represents historically recorded maximum and minimum since 2016. Data recorded during COVID period was lover in 5% of tested days, but in most cases -52% of tested days- it was higher than historically registered levels. Hot spring of 2020 affected lower, but still historically registered demand. The curve is located at the bottom of the benchmark channel [7]. Extremely frosty end of winter 2021 [8] was the reason for record-breaking demand for natural gas in February and April. It is important to underline that COVID did not reduce consumption and during tested period higher levels of demand for natural gas were registered on end users connected to distribution system.

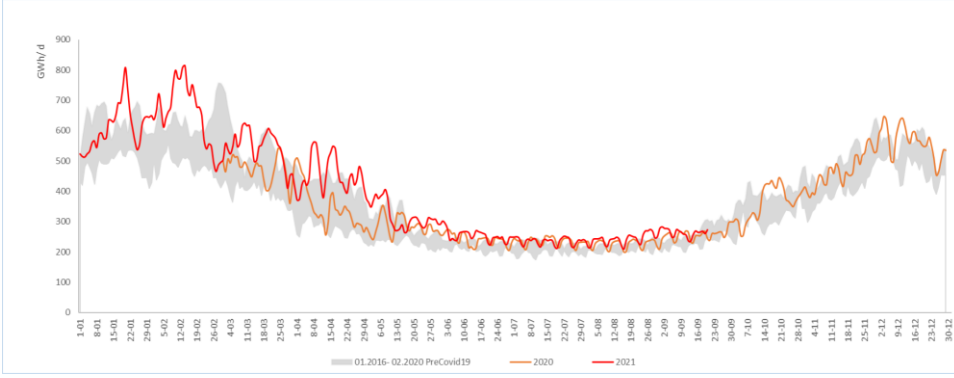

Fig. 1. End users demand for high methane natural gas on the distribution system.

4.2 Transmission System

Figure 2 represents the natural gas demand registered by end users connected to the transmission system. Flat shape of historical channel and flat curves of 2020 and 2021 demand were expected. Data recorded during COVID period was lover only in 1 tested day, in 69% of tested days it was higher than historically registered levels.

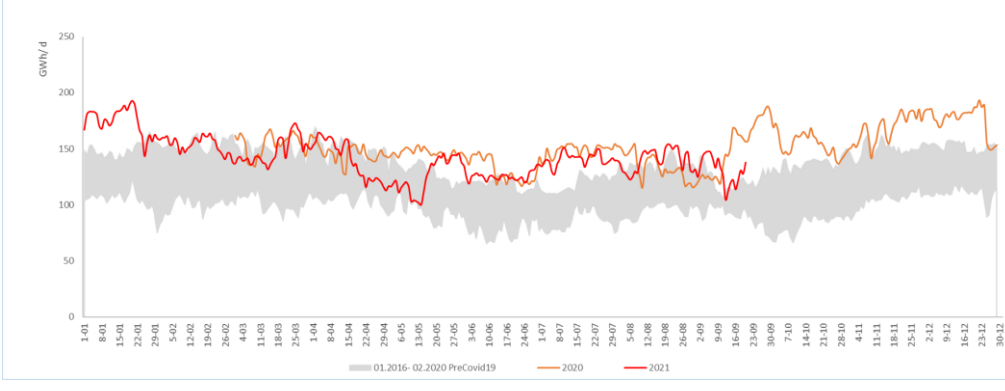

Fig. 2. End users demand for high methane natural gas on the transmission system.

However weeks that are different from the others can be observed. The April and May 2021 data are located at the bottom of historical channel. Transmission system end users demand is temperature resistant, so temperature cannot be the reason. Prices of electricity and gas were also predictable in this period, and carbon dioxide emission were expensive, so this should promote the production of electricity from gas. What is interesting: this short period with lower gas demand coincides with the second significant wave of COVID cases registered in Poland. This is the only period in which the pandemic could have had an impact on gas fuel demand.

4.3 Security of supply and underground storage facilities

It is necessary to mention about underground gas storage facilities. Due to the hot spring in 2020, withdrawal season has ended earlier with higher inventories of gaseous fuel. This made it possible to complete the injection season in September 2020, so more than a month earlier than

usual. 2021 inventories are located in the middle of the historically based tunel. Data of natural gas stocks is presented in Figure 3.

It is worth pointing out that the gas storage facilities are filled in Poland on highest levels on whole European Union. At the end of 30.09.2021 gas day all underground gas storages located in the European Union were 74,62% full. UGS connected to the Polish transmission system were 96,29% full. [10]

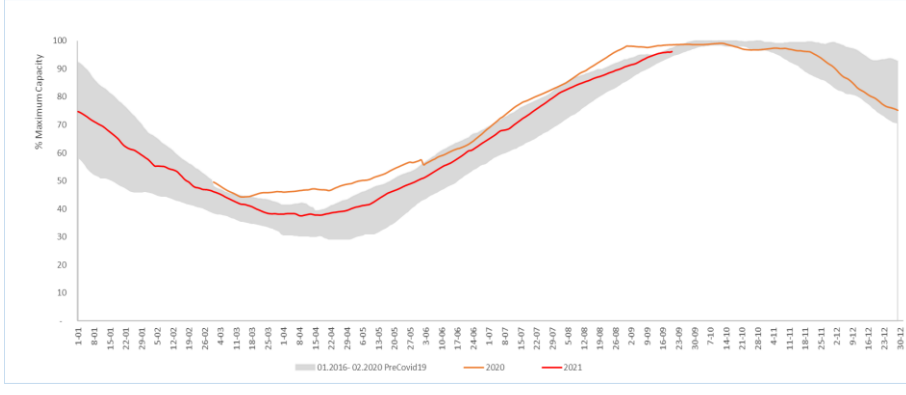

Fig. 3. Inventories of high methane storage facilities.

4.4 Comparison of development plan and measured demand

Every 2 years Transmission System Operator in Poland is obliged to publish network development plans for the next 10 years. The last publication before global pandemic took place in April 2019. The forecasts published then are represented by green curves on the graph - Figure 4. The red curve is the measured and confirmed values of the natural gas demand. What is easy to observe that 2019 was already overestimated, which resulted in the difference in the plan and demand in 2020 also. After the full 9 months of 2021 and on the base of historical development dynamics three forecast of demand were calculated.

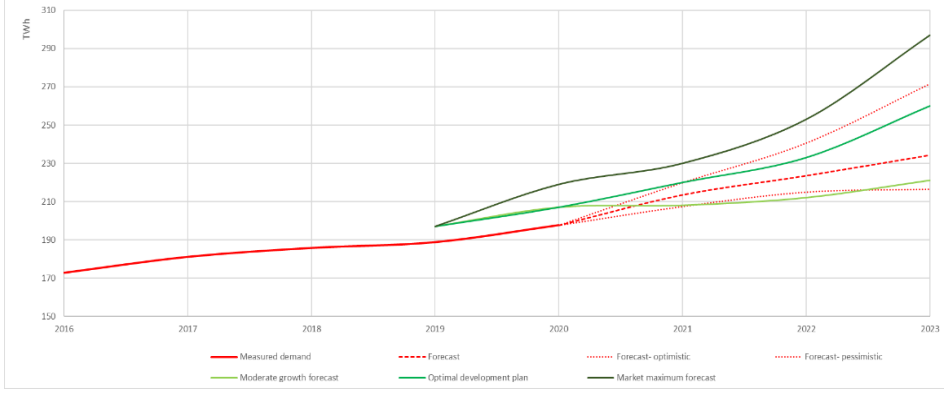

Fig. 4. Development plans

Calculated pessimistic scenario will cross the moderate growth forecast at the end of this year. The development scenarios are still valuable and still can be used for market analysis.

5. Conclusions

The Polish natural gas sector during the tested period was immune to the impact of the global COVID-19 pandemic. Volumes of natural gas used by industrial and private end users are still increasing. Further analysis of the impact of the pandemic on the natural gas sector, due to the increasing gas prices seems to be pointless. Gas price was one of the five indicated primary consumption drivers. On the Polish market price registered for 30.09.2020 DA product was 66,11 [PLN/MWh]. Twelve months later, the price was higher and for 30.09.2021 DA product was 390,56 [PLN/MWh] [14]. Low level of natural gas inventories in European UGS and cold winter 2021 may contribute to high prices until spring of 2022. Global changes in the gas market mean that prices will be the main factor creating demand in the nearest future. The development plan established before the pandemic are implemented in accordance with the assumptions of 2019.

References

[1] European Commission, Quarterly Report Energy on European Gas Markets with focus on the impact of Covid-19 on the global LNG market, Market Observatory for Energy, Volume 13, 2020,
[2] International Energy Agency, Gas 2020 Report, IEA Publications, 07.2020, p.6-16.
[3] Koronawirus odciążył sieci. Zużywamy mniej prądu, money.pl; 2020 [accessed 15.10.2021],
[4] Gaz-System, Zdolność przesyłowa; https://www.gaz-system.pl/strefa-klienta/system-przesylowy/zdolnosc-przesylowa/; 2021 [accessed 21.09.2021],
[5] Schuster T., Bogucki A., Monitoring parametrów cieplnych gazu ziemnego w systemach dystrybucyjnych w kontekście rozliczeń energetycznych, Nafta- Gaz, nr 9, 2012,
[6] Kumor M., Porada S. A common gas market for Visegrad Group countries. Eastern Review 2020; t. 9, s. 131–148. DOI: 10.18778/1427-9657.09.09,
[7] Ciepły marzec 2020, choć bez ekstremów, https://meteoprognoza.pl/; 2020 [accessed 15.10.2021]
[8] Najzimniejszy kwiecień w tym wieku, https://meteoprognoza.pl/; 2021 [accessed 15.10.2021]
[9] Bąkowski K. Sieci i instalacje gazowe, PWN; Warszawa 2014,
[10] Aggregated Gas Storage Inventory, https://agsi.gie.eu/#/; 2021 [accessed 21.09.2021]
[11] krajowy dziesięcioletni plan rozwoju systemu przesyłowego, kwiecień 2019,
[12] Krysa Z. Obliczanie i kształtowanie się spreadów na rynkach energii, Polityka Energetyczna, Tom 13, 2010
[13] Sprawozdanie z działalności Prezesa Urzędu Regulacji Energetyki w 2020 r., Warszawa, 2021
[14] TGE Natural Gas Index TGEgasDA, https://tge.pl/; 2021 [accessed 15.10.2021].

FUEL VAPOR CANISTER AS AN ENVIRONMENTALLY ESSENTIAL ELEMENT OF GASOLINE CARS

Natasza Rutkiewicz[1,3], Sylwia Turniak-Kwarciak[1,3], Andrzej Kalina[3], Mariusz Macherzynski[2*]

[1] Doctor School of AGH University of Science and Technology, Al. Mickiewicza 30, 30-059 Krakow
[2] AGH University of Science and Technology, Department of Coal Chemistry and Environmental Sciences, Faculty of Fuel and Energy, Al. Mickiewicza 30, 30-059, Krakow
[3] BorgWarner Mobility, ul. Wielicka 28B, 30-552 Kraków
* corresponding author: macherzy@agh.edu.pl

Abstract. *The article acquaints the reader with the current state of knowledge about fuel vapor canisters used in gasoline vehicles. It explains what this element of the vehicle is, why it is important for the human environment and what kind of research is carried out or implemented to optimize these elements - also using the examples of research performed by the authors. The implementation of outlined topic is an example of good cooperation between industry and technical universities in Poland.*

Keywords: *fuel canister, gasoline, hydrocarbon emissions, carbon adsorption materials, carbon monolith.*

1 Introduction to fuel vapor canisters, environmental importance

The carbon canister or just canister is a very important, key element of emission control in gasoline cars. The canister is a non-serviceable part that is crucial for the homologation process. Car manufacturers cannot market the new model without positive test results for this component.

Hydrocarbons (HCs) from fuel vapours are classified as volatile organic compounds, the so-called VOCs. They pollute the air, are toxic to living organisms and take an active part in the formation of photochemical smog. In Poland, according to the report of the Supreme Audit Office (NIC): "Elimination of vehicles from road traffic excessively emitting harmful substances" [1], hydrocarbons constitute 45.3% of substances contributing to smog production. In line with the global trend, the emission standards are being lowered more and more, which automatically forces the optimization of the existing canisters [2].

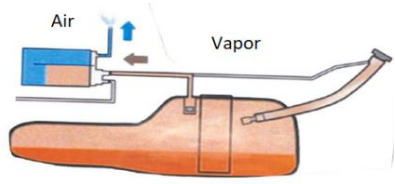

Fig. 1. Diurnal emissions from vapour canister.

In simply terms, each canister consists of a plastic housing containing one or more chambers (usually three) filled with activated carbon in various forms, which is designed to adsorb and store excess of hydrocarbon vapours. HCs can be generated by fuel (gasoline) during several evaporation processes, which include [3]:

- diurnal emissions: result of fuel evaporation during daily temperature fluctuation (Fig. 1),
- running loss emissions: fuel vapor emissions during operation of the fuel system (car driving), when the engine and exhaust gas temperature increases and is high,
- hot soak emissions: these are the emissions that occur within the first hour after the car is parked when the engine is no longer running but still emitting heat,
- refuelling emissions: occurs during refuelling a car, when the fresh fuel pumped into the fuel tank displaces the hydrocarbon-rich vapours already present (Fig. 2).

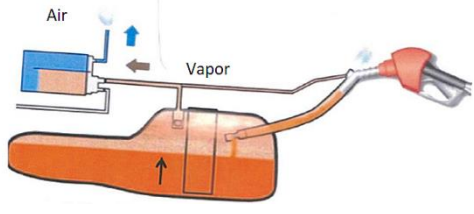

Fig. 2. Refuelling emissions from vapour canister.

2 Mode of operation of canisters, features of carbon filling materials, applicable legal standards age layout

The carbon in the canister can be in the form of granules or pellets. It is an amorphous and non-polar material with a very high ratio of adsorption area to volume. It has three types of irregularly shaped pores: mesopores with a diameter (r) range from 2 nm to 50 nm (slightly larger than typical fuel hydrocarbon molecules in a tank), micropores ($r < 2$ nm) and macropores ($r > 50$ nm). This material is able to temporarily trap fuel originating HCs, coming in a form of flowing vapours with other gases. For this process, the mesopores are most important because they ensure an optimal equilibrium between the adsorption and desorption processes. While coming to the canister through the tank port, HC molecules condense on the surface of the adsorbent inside the pores using weak intermolecular (van der Waals) interactions. During reverse purge, the stream of air flows in through the air port (tube) and desorbs the HCs, directing vapours to the purge tube, through which they are drawn into the engine in a limited amount (Fig. 3). In other words, the canister is connected to a port with the engine's intake manifold by means of a solenoid valve, and under the right conditions, when the inflow of fuel vapor does not deteriorate engine's operation, the valve opens to regenerate the canister. Negative pressure causes a large amount of ambient air

to flow back through the adsorbent beds, overcoming the van der Waals interactions and desorption of HCs particles as well as their sucking into the engine and final combustion.

As a result of repeated canister charging and cleaning cycles, a HCs concentration gradient appears in the activated carbon bed, with a higher concentration near the tank port and a lower concentration towards the air tube. Adsorbed HCs, especially the lightestones, tend to diffuse from high concentration areas to the lower concentrated. The process of capturing HCs will continue until the carbon bed is saturated and breakthrough occurs i.e., HCs particles are no longer adsorbed and pass through the absorber to enter the atmosphere. In the automotive industry this stage is defined as breakthrough, which is the moment when 2 g of HCs is emitted

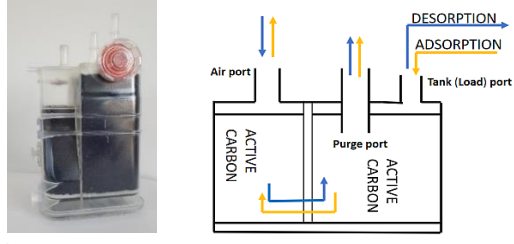

Fig. 3. Vapour canister (left) and its operation diagram (right).

outside the canister. The daily heating of the fuel tank causes a small air leak from the fuel tank through the canister, which carries a small number of HCs with it. These are the so-called bleed emissions that occur before the final breakthrough.

The US has the most stringent regulations on EVAP (the Evaporative Emission Control System) emissions, where the canister bleed test [4] limit is 0.020 g/test. The China 6 EVAP limit is 0.7 g/test within 2 test days, however this test has a higher conditioning temperature (38 ± 2^0C). The Brazilian PROCONVE L7 (January 1, 2022) sets the EVAP emission limit to 0.5 g/test within 2 test days. At this moment the limit for Euro 6 is 2 g/test. These ever-increasing demands on emissions are prompting automotive component manufacturers to optimize their existing products, both in terms of construction e.g.: change of the number of chambers, use of “air gaps", different arrangement of carbon in the chambers or the use of new solutions related to the introduction of new materials. Further challenges include hybridization and partial electrification of cars, which reduce fuel consumption, but require that the canister must operate under reduced or even no blow-by conditions (closed fuel systems NIRCO [5]). Canisters as one of the components of the car must meet the emission but durability requirements too. They have to work throughout the expected service life of the vehicle, which is currently assumed for most cars as 15 years or 150,000 miles (240,000 km), depending on which of these values will be reached later.

3 Examples of fuel canister tests

Meeting the conditions pointed out in Chapter 2 requires understanding how the efficiency of the canisters as a component of the EVAP system is related to the characteristics of activated carbon (chemical composition, sorption capacity, pore size distribution, grain diameter or size). Also, a broadly understood characteristics of canisters (type, geometry, loading speed, rinsing speed, restrictions) is important. Optimizing canisters requires exploring many potential ways and solutions to improve their performance, and all research must take into account the final ecological

as well as economic aspects of these activities. One of the contemporary solutions is the use of other types of carbon adsorption materials, such as monoliths (carbon profile usually in the form of a cylinder with many parallel channels) – Fig.4. Monoliths can be used as one of the end elements of the canister. It is an alternative part made of an adsorptive material with different properties ensuring greater efficiency of the canister as a whole).

3.1 Tests no. 1

An example experiment is presented, which allows to compare the mode of operation and effectiveness of commercially used monoliths (sample B) and newly tested one (sample A). Cylindrical monoliths having the same diameter of 29 mm and a length of 100 mm were selected. Both monoliths had the same low carbon content comparing to ceramics. Selected monoliths were conditioned with n-butane (standard gas simulating gasoline vapours) and back air purge (150 and 750 sL - standard litres). 3 cycles of n-butane charging (mixture with nitrogen until 2 g breakthrough) and 3 cycles of air purge were performed (one after each charging). Then, samples were prepared from 3 slices (I, V, X) of the monolith, 5 samples (1-5) representing the interior and 4 samples (I-IV) taken from the skin layer, according to the scheme presented in Fig. 4.

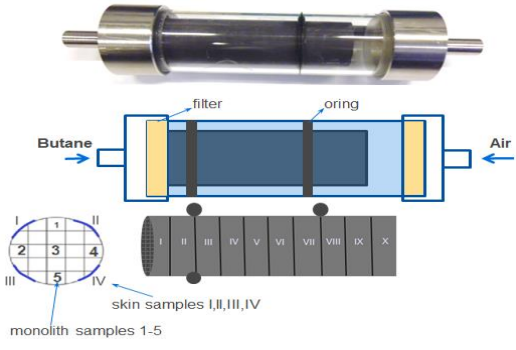

Fig. 4. Scheme of monolith preparation for conditioning and sampling prior GC-MS analysis.

The collected samples were placed in vials and chemical analysis was performed using a GC-MS system equipped with an automatic headspace sampler (HS-sampler). A simplified diagram of devices is shown in Fig. 5. An FID detector was not used in these experiments.

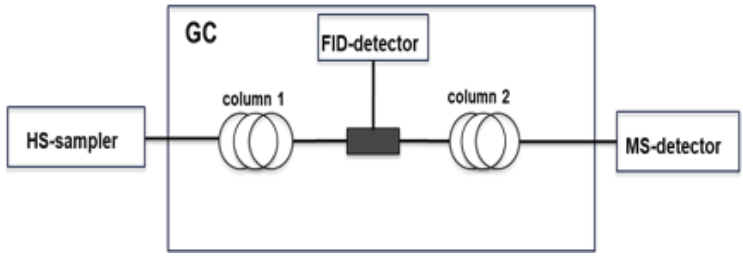

Fig. 5. HS-sampler / GS / MS system operation diagram used for chemical analyses, description in the text.

The vials with samples were placed in the autosampler and subjected to temperature stabilization. After incubation each gas sample was taken above the monolith fragment and analysed by GC-MS. These studies allowed the comparison of the effect of purge on post-

breakthrough regeneration of carbon adsorbent material. The quantity of HCs (HCs SUM – sum of the area of HCs chromatographic peaks) still remaining in the mass unit of the material was measured after all three cycles were performed. This makes it possible to initially compare the materials with each other - lower residual amounts mean better purging efficiency. Thanks to this, it is possible to perform an initial classification of selected monoliths in terms of their suitability in fuel vapor absorbers. The test no.1 results are summarized in Table 1.

The comparison of the data reveals that with the same purge parameters, monolith B regenerates much better in each tested layer. There are the residual concentrations at least 50% lower in the material B slides for both purges. In extreme cases, in monolith B there was 25-33% of the quantity of HCs remaining in monolith A. Additionally, the lower residual concentrations are observed along each monolith from the air tube side (slide X), which indicates a potential for better cleaning of monoliths but with prolonged purge.

Table 1. Residual HCs concentrations in slides of monoliths A and B after air purging with 750 and 150 sL.

MONOLITH A	**PURGE**					
	750 sL			**150 sL**		
Monolith slide	Internal HCs [SUM/g]	Skin HCs [SUM/g]	Slide Total HCs [SUM/g]	Internal HCs [SUM/g]	Skin HCs [SUM/g]	Slide Total HCs [SUM/g]
I	8	9	17	20	29	48
V	6	6	12	21	26	46
X	4	4	8	18	22	39
MONOLITH B	**PURGE**					
	750 sL			**150 sL**		
Monolith slide	Internal HCs [SUM/g]	Skin HCs [SUM/g]	Slide Total HCs [SUM/g]	Internal HCs [SUM/g]	Skin HCs [SUM/g]	Slide Total HCs [SUM/g]
I	4	4	8	10	8	18
V	3	3	6	10	7	17
X	1	1	3	7	6	13

3.2 Tests no. 2

Other tests allowed to assess whether there is a relationship between the thickness of the monolith's outer wall (skin) and the level of HCs removal from the entire fitting during purging process. This is an important example of how the size of the structure can result in better performance under the same operating conditions of the monolith. Test monoliths made of material promising hope for wider use in canisters were selected. The fittings selected for the tests had the same diameter (29 mm) and length (100 mm), while three different wall thicknesses. The monoliths had the same carbon content of 60%. The sample preparation and analysis procedures were the same as for the purging effect study (Chapter 3.1). The data is shown in Fig. 6. As the result, the total mass of the HCs realised from all the 27 samples taken from three slides, after charge/purge cycles, was calculated. It was converted to 1 g of the sampled material (residual HCs concentration).

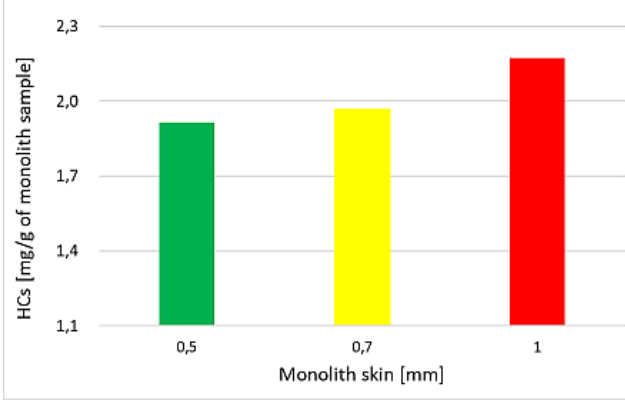

Fig. 6. Dependence of the residual HCs concentration in monoliths on the thickness of their skin.

The research proved that the thickness of monolith skin had a significant influence on the purging process efficiency. The thicker the skin, the worse the purging of the monolith, and the greater the quantity of HCs left in the material, resulting in higher emissions. It can be assumed that the responsible for this is the limited diffusion of HCs from thicker layers of the tested carbon material.

4 Conclusions

The presented topic of fuel vapor canisters is closely related to the human natural environment protection and is in line with the most important trends in environmental research in the era of decarbonisation and zero-emission technologies.

The exemplary laboratory - analytical tests presented in the paper allow for the preliminary classification of the tested monoliths for wider use in fuel vapor canisters with limited purging parameters.

The described work will be extended by the development of further tests of canisters of various types and designs and their components. The preparation of a full range of tests and studies requires a lot of work to refine the methodologies and improvements. There is an enormous potential and need, as well as many possible applications, which mainly applies to:

- quick and cheap verification of new adsorptive materials, potentially important for the development of canisters,
- quick verification of operation and effectiveness of already used carbons, monoliths and other adsorptive materials,
- gaining information on the effectiveness of HCs purging from canister materials, which is very important for their emission to the environment.

The described field of research is carried out in the framework of two doctoral dissertations conducted in cooperation between AGH UST and the BorgWarner company. There was a need to launch by the company a RD laboratory located at AGH, enabling the planning and performance of most research. Scheduled work includes the elaboration and development of methods for analysing emissions from canisters. The use of specially constructed test stands in conjunction with gas chromatography (GC) with MS/FID detection and headspace analysis will enable the measurement of emissions from the adsorbent material as well as the quantitative and qualitative

evaluation of the emissions from the canisters under simulated operation in the vehicle fuel system. Actions will be taken to optimize the absorbers in terms of materials and construction in order to reduce emissions and production costs, as well as to meet global emission standards for these car components.

Acknowledgements

The work was co-financed by a Dr. Macherzynski subsidy (Faculty of Energy and Fuels, AGH UST no. 16.16.210.476 B02).

We would also like to thank the management of BorgWarner and previously Delphi Technology for their involvement by offering employees to conduct research in the newly opened BorgWarner RD laboratory at the AGH UST, under two doctorates financed by MEiN (Polish Ministry of Education and Science) being pursued, including one implementation doctorate ("doktorat wdrożeniowy").

References

[1] Informacja o wynikach kontroli NIK: Eliminowanie z ruchu drogowego pojazdów nadmiernie emitujących substancje szkodliwe, https://www.nik.gov.pl/plik/id,23218,vp,25925.pdf, 2020, [accessed 3.11.2021].

[2] Delphi Technologies booklet: "Worldwide emissions standards passenger cars and light duty vehicles", 2019/2020.

[3] The internal training of BorgWarner company, 2020.

[4] Williams R.S. and Reid Clontz C. Impact and Control of Canister Bleed Emissions. SAE Transactions, vol. 110, Section 4: JOURNAL OF FUELS AND LUBRICANTS (2001), pp. 579-587, https://www.jstor.org/stable/44742670 [partial access 3.11.2021].

[5] A. Kalina (Delphi Techn. Group). Evap Canister Developments to Meet Emission Targets and Powertrain Trends, oral presentation in ITB Group Conference: Automotive Energy Storage Systems, 04-05.03.2020, Novi, Michigan, USA, not published, https://www.itbgroup.com/automotive-energy-storage-systems-2020/, [access to the conference agenda 3.11.2021].

ISBN: 978-83-66559-07-3